POSTPARTUM CERVICAL REPAIR IN *MUS MUSCULUS*: POTENTIAL ROLE FOR VASCULAR ENDOTHELIAL GROWTH FACTOR AND HYPOXIA INDUCIBLE FACTOR 1 ALPHA IN CERVICAL WOUND HEALING

A Thesis
by
ROBERT LEE STANLEY

Submitted to the Graduate School
at Appalachian State University
in partial fulfillment of the requirements for the degree of
MASTER OF SCIENCE

May 2013
Department of Biology

POSTPARTUM CERVICAL REPAIR IN *MUS MUSCULUS*: POTENTIAL ROLE FOR VASCUALR ENDOTHELIAL GROWTH FACTOR AND HYPOXIA INDUCIBLE FACTOR 1 ALPHA IN CERVICAL WOUND HEALING

A Thesis
by
ROBERT LEE STANLEY
May 2013

APPROVED BY:

Chishimba Nathan Mowa, Ph.D.
Chairperson, Thesis Committee

Sue Bauldry, Ph.D.
Member, Thesis Committee

Guichuan Hou, Ph.D.
Member, Thesis Committee

Susan L. Edwards, Ph.D.
Chairperson, Department of Biology

Edelma D. Huntley, Ph.D.
Dean, Research and Graduate Studies

Abstract

POSTPARTUM CERVICAL REPAIR IN *MUS MUSCULUS*: POTENTIAL ROLE FOR VASCULAR ENDOTHELIAL GROWTH FACTOR AND HYPOXIA INUCIBLE FACTOR 1 ALPHA IN CERVICAL WOUND HEALING

Robert Lee Stanley
B.S., Appalachian State University
M.S., Appalachian State University

Chairperson: Chishimba Nathan Mowa, Ph.D.

Cervical remodeling (CR) is the active process where the birth canal prepares for parturition. CR is divided into four distinct yet overlapping phases, with the first three phases taking place during gestation and parturition, whereas the fourth and final phase, postpartum repair, ensures proper healing and recovery of the cervix back to a non-pregnant state. Postpartum repair is the least studied phase of CR, and to date, this is the only study of which we are aware that focuses exclusively on postpartum repair. Here, we examined the gross and ultra-morphological changes taking place in the cervix during the first 48h postpartum, the expression profiles of four key proteins: vascular endothelial growth factor (VEGF), hypoxia inducible factor 1 alpha (HIF-1α), and two VEGF receptors (KDR and Flt-1), and using quantitative proteomics, we sought to determine the genome-wide protein expression patterns taking place in the cervix during the least studied phase of cervical remodeling. From these studies, we demonstrate 1) the cervix undergoes vast morphological changes during the first 48h postpartum, 2) HIF-1α, VEGF, and its receptors KDR and Flt-1 are readily expressed at both the gene and protein levels, and 3) quantitative proteomics revealed dynamic changes in several cytoskeletal elements as well as immune-related proteins.

Dedication

I wish to dedicate this work to my late grandfather Winton "Pop" Poole. He began his life working as an auto mechanic, was drafted towards the end of WWII, and when finished with his service to his country, he worked his way up from a bank teller to Vice President of Marketing for Nations Bank (Bank of America). Education was very important to him, as such he made sure that his two daughters went to college, and he made college savings accounts for his four grandchildren. In the weeks before I began college in 2005, he told me two pieces of wisdom which I took to heart then, and their meaning has not lessened over the years "in this day and age, with all the resources available, there is no reason anyone should stop their quest for knowledge" and "if you work 10% harder, you are working harder than 95% of the population." Thank you for your wisdom and love; my only regret is that Pop did not live long enough to see his grandson gain acceptance to medical school.

I also wish to dedicate this work to my best friend, wife-to-be, and the future mother of my children, who will become all too familiar with cervical remodeling, Stephanie Leemhuis. I am a better man because of you. Thank you for being with me during the best and worst of times. You are the love of my life, and I cannot wait to grow old with you.

Acknowledgments

I would like to acknowledge the following sources of funding for this study: Appalachian State University office of student research, Cratis D. Williams Graduate School, and the Sigma Xi Scientific Research Society. I wish to acknowledge Dr. Chishimba Nathan Mowa for his patience, guidance, and wisdom since I met him during my last semester of my undergraduate career. I would also like to acknowledge the GRAM program, which Dr. Mowa received and selected me as the recipient. I wish to acknowledge and thank my colleagues in our research lab, Siobhan Donnelly, Jordan Estes, Takako Ohashi, Molly Fike, Benjamin Coe, and Susan Zhao. Thank you for your help, encouragement, and friendship. I would like to acknowledge my thesis committee members, Dr. Sue Bauldry and Dr. Guichuan Hou for their assistance during my graduate career. I wish to acknowledge Ms. Monique Eckerd, for her help in the animal facility, as well as generously donating time-pregnant mice used in this study. I wish to thank my friends (you know who you are) and my family, Stephanie, Mom, Dad, Gran, Drew, Lauren, and all other family members for their love and support.

Table of Contents

List of Figures

Foreword

The research described in this thesis will be submitted to *Biology of Reproduction*, the official peer-reviewed journal of the Society for the Study of Reproduction. The in text citations as well as the references of this thesis have been prepared according to the style guide for the journal.

Introduction

The cervix undergoes marked changes during pregnancy, parturition (birth process) and postpartum (immediately after birth) [1]. Alterations linked to pregnancy enables the cervix to provide mechanical resistance to the increasing gravitational force exerted on it by the fetus, and thus ensures that the fetus is held *in uterine* [1], whereas at parturition, the cervix becomes malleable and dilates to allow passage of the fetus through the birth canal [2]. Immediately following birth, the cervix undergoes an extensive reconstruction and healing phase that restores it to its non-pliable and non-pregnant state [3]. Collectively, these changes are termed cervical remodeling [CR], which is divided into four distinct yet overlapping phases, namely softening, ripening, dilation, and postpartum repair [4, 5]. To date, most of the studies have focused on the first three phases of CR, almost to the exclusion of the fourth phase, postpartum repair.

Postpartum repair (sometimes termed reconstruction) consists of a set of complex biological processes that will ultimately restore the cervix to its original non-pregnant state, and thus ensure normal cervical function for subsequent pregnancies [1, 2]. This final phase of CR is generally characterized as an inflammatory and wound healing response [3, 6], as demonstrated by studies that utilized gene microarrays. These studies have shown that a variety of factors, including pro-inflammatory factors, metalloproteases, proteins involved in extracellular matrix (ECM) synthesis, and genes governing epithelial differentiation pathways are all upregulated postpartum [3, 7]. Immune cells, including neutrophils, eosinophils, and both M1 & M2 macrophages, have all been shown to increase postpartum compared to earlier phases of remodeling [1, 2, 8]. This inflammatory response could serve to promote repair of the

cervix after parturition and/or serve a protective role for the birth canal against environmental hazards, such as infection [7]. Because inflammation and wound healing are intricately linked to vascular events, factors that regulate this process, notably vascular endothelial growth factor (VEGF) [9], also likely influence postpartum cervical repair.

VEGF belongs to the platelet-derived growth factor family and has a variety of well characterized functions, including vasculogenesis, angiogenesis, and endothelial cell mitogenesis. It is also a chemo-attractant for immune cells [10-13]. VEGF exerts a variety of biological effects in the cervix, including regulation of cell proliferation, tissue remodeling, induction of inflammation, cervical epithelial growth, immune cell recruitment, and CR [9, 14-15]. VEGF exerts its biological effects and elicits cellular responses through binding to two receptor tyrosine kinases, termed Flt-1 and KDR/Flk-1 [12, 16]. Numerous isoforms of VEGF derived from alternative RNA splicing have been identified, denoted as VEGF-xxx, where xxx is the number of amino acids of the mature protein [17, 18]. The most abundant isoform in humans is VEGF-165, which corresponds to VEGF-164 in rodents. The normal rat cervix expresses both receptors of VEGF (KDR and Flt-1) and three VEGF isoforms, namely 120, 164 and 188, with 164 being the most prominently expressed [19].

The importance of VEGF's role in wound healing has been well documented and characterized [20-23]. VEGF controls wound healing by inducing various vascular processes, including angiogenesis (capillary growth), vaso-permeability, recruitment of immune cells, as well as epithelization and collagen deposition [23], which is a hallmark of the healing response [2]. For instance, induction of capillary growth during wound repair helps meet the high demand for oxygen and nutrients, as well as removal of waste products [22]. Indeed, inhibition of angiogenesis impairs wound healing, demonstrating the vital role of VEGF in this (healing) process [20, 23]. Factors that induce VEGF expression during wound healing include growth factors (transforming growth factor, hepatocyte growth factor, keratinocyte growth factor, etc.),

pro-inflammatory cytokines (IL-1, TNFα), and hypoxia (low oxygen) [13]. Cells in a hypoxic environment will accumulate the intracellular transcription factor hypoxia inducible factor 1 alpha [HIF-1α] which is the most potent inducer of VEGF transcription [24]. Following injury, VEGF is first secreted by hypoxic cells and will establish a gradient of VEGF mirroring the gradient of hypoxia [22]. Activated platelets and immune cells, i.e. macrophages and neutrophils, express Flt-1 and respond chemotactically to VEGF and will migrate towards the VEGF source at the site of injury and/or hypoxia [13, 23]. Macrophages and neutrophils will, in turn, stimulate angiogenesis by further secreting VEGF and TNFα that will also stimulate VEGF production in keratinocytes and fibroblasts [23]. Although VEGF's role in the cervical events during pregnancy has been studied, to date, no study has examined its role, if any, in postpartum cervical repair.

Given the facts that postpartum repair is characterized as a pro-inflammatory wound healing response [2, 3, 6], and that VEGF induces inflammation in the cervix [9] and plays roles in **a)** cervical remodeling leading up to pregnancy in rodents [14, 15], and **b)** general wound healing [13, 23], we can speculate that VEGF plays a role in the postpartum repair phase of CR. In this study, we sought to determine **1)** the gross morphological changes of the cervix postpartum, **2)** the expression patterns of HIF-1α, VEGF, and the VEGF receptors Flt-1 and KDR, during the first two days of postpartum repair in mice and, **3)** potential roles of these proteins through proteomics analysis.

Materials and Methods

Animals and Postpartum Time Intervals

Pregnant wild type (WT) mice (C57BL6/129SvEv; Charles River, n= 3) were used for all the groups in the present study. The time of the first pup noted as time 0hr and the mothers were sacrificed at an 8h interval, after parturition, beginning with 0h, i.e. 0, 8, 16, 24, 32, 40, and 48h. All animals were euthanized by a lethal injection of sodium pentobarbital (150mg/kg bw, i.p.) and transcardially perfused with 0.9% saline solution. Cervices were harvested carefully under a stereomicroscope to avoid contamination with vaginal and uterine tissues, and the cervices were then processed and analyzed according to imaging, gene, and protein expression protocols. All animals were housed under the following conditions: constant room temperature, a 12:12 light and dark cycle, and free access to water and food. All experiments were performed in accordance with the *Guide for the Care and Use of Laboratory Animals* of Appalachian State University and the NIH guidelines (NIH publication number 86-23), with efforts made to minimize both number of animals used and animal suffering.

Scanning Electron Microscopy (SEM)

SEM was employed to observe the surface of cervical epithelia and any changes occurring during the postpartum period. Harvested cervices were immediately immersed in a 2.5% glutaraldehyde, 0.1M phosphate buffer solution (PBS), and the tissues were then dehydrated in a graded series of ethanol and dried using a critical point drying apparatus (Polaron Instruments Inc.). The dry samples were mounted on aluminum stubs with carbon adhesive paper, sputter coated in gold, and viewed with the SEM (FEI Company). The cervical

epithelium was evaluated for various features, including, but not limited to involutions, tissue size, overall appearance of cells, mucus, ECM molecules, and para-cellular spaces.

Hematoxylin and Eosin (H&E) Staining

H&E staining was utilized to complement the SEM data, as well as to observe any morphological changes happening in the underlying connective tissue of the cervix. Harvested cervices were immersed in a 10% formalin, pH 7.2, aqueous solution. The tissues were fixed in formalin at 4°C for 3-4 days and first transferred into saturated sucrose dissolved in 0.1M PBS, for at least 2 days prior to sectioning (12um) with the Cryostat (Leica) at -30°C. After sectioning, the slides were either stained immediately or stored at -20°C until staining. For staining, first, the sections were washed in distilled water, stained with Harris hematoxylin solution for 8min, and washed in running tap water for 5min. Next, slides were placed into 1% acid alcohol differentiation solution for 30sec, washed in running tap water for 1.5min, and placed in a clarifier solution for 15sec. Then, the slides were washed in running tap water for 5min, rinsed in 95% alcohol, before counterstaining with eosin-philoxin solution for 42sec. Then, slides were dehydrated in 95% and two changes of 100% alcohol for 5min each, and cleared with xylene. Finally, slides were mounted with xylene based mounting medium, and viewed on an inverted microscope (Olympus IX81).

Gene Expression (Real-time PCR)

To perform gene expression studies the mRNA was first extracted, reverse transcribed into cDNA, and then amplified as described below. Harvested cervices were snap-frozen. Then, either RNA was extracted immediately or the tissues were stored at -80°C until processing. Total RNA was extracted, and its quality and quantity were determined using the Nano drop apparatus (Thermo Scientific). If the RNA was of good quality and quantity, the RNA (1000ng)

was first, reverse transcribed using a cocktail containing the following: $MgCl_2$, reverse transcriptase, RT buffer, dNTP, RNase inhibitor, RNase-free water, and random hexamers, in order to generate an equivalent amount of total cDNA using a thermo cycler (Eppendorf) at the following settings: 25°C for 10min, 42°C for 2h, 95°C for 5min, and 4°C for storage, according to protocol. Next, the cDNA was used to amplify specific gene sequences using real-time PCR amplification (e.g. HIF-1α, VEGF, Flt-1, KDR, and Gus-β as a normalizer) in order to determine the relative expression of these genes throughout postpartum. We used commercially pre-designed and optimized real time PCR probes (Applied Biosystems). The PCR reaction was set up in 96 well plate in a volume of 25μL per well, with the following components: 5μL of cDNA, 12.5μL of 2x Taqman Universal PCR Mastermix, 1.25μL of 20x Assays-on-demand Gene Mix (e.g. VEGF), and 6.25μL of RNase-free water. Finally, DNA amplification was performed using the Applied Biosystems Real-Time PCR machine (ABI 7300 HT) with the GeneAmp 7300 HT sequence detection system software (Perkin-Elmer Corp.) with the settings as follows: 95°C for 10min, and then 40 cycles of 95°C for 15sec, and 60°C for 60sec.

Western Blot

Western blot analysis was used to confirm relative amounts of the proteins of interest, at the tissue level. Harvested cervices were snap-frozen and stored at -80°C until processing. Total protein was extracted and quantified with a BCA assay (Thermo Scientific). Next, the protein samples, along with a set of standard protein ladders (Bio-Rad), were loaded on a 4-12%Bis-Tris Gel (Invitrogen). The gel was electrophoresed at 75V until the dye was close to the bottom of the gel. Thereafter, the protein was transferred to a PVDF membrane using the iBlot apparatus (Invitrogen), and the membrane was incubated overnight with Blotto (5% dehydrated milk in Tris Buffered Saline with Tween) solution at 4°C. The following day the membrane was incubated with the diluted primary antibody (1:1000 dissolved in Blotto; Santa

Cruz Biotech, sc-130656, sc-10790, sc-507, sc-316, sc-504), and left to incubate overnight on a shaker at a constant room temperature (20°C). Thereafter, the membrane was washed three times in 1X TBST for 20min, after which the membrane was incubated with the secondary antibody (1:10,000 in TBST, Santa Cruz Biotech, sc-2313) for 1h at 20°C on a shaker. First, the membrane was washed three times with 1X TBST and one wash with 1X TBS. Next, horseradish peroxidase (HRP) solution was added to the membrane for 5 min, and the excess solution was dripped off. Finally, the membranes were exposed to x-ray film (GE) in a dark room for optimum times (~ 30sec – 1min), and the film was developed and analyzed for presence of target proteins (HIF-1α, VEGF, Flt-1, KDR, and β-actin as a normalizer). The densitometry was quantified using ImageJ software.

Confocal Immunofluorescence

Confocal immunofluorescence was employed to complement Western blot data of the proteins of interest (HIF-1α, VEGF, and VEGF receptors) as well as cellular localization in the cervix. Harvested cervices were immersed in a 10% formalin (pH 7.2) aqueous solution. The tissues were fixed in formalin at 4°C for 3-4 days and then transferred into saturated sucrose dissolved in 0.1M PBS, for at least 2 days prior to sectioning (12μm) with the Cryostat (Leica) at -30°C. After sectioning, the slides were either stained immediately or stored at -20°C until staining. For staining, the sections were initially incubated with 10% normal goat serum in 0.1M PBS for 20min at 20°C in order to block non-specific protein binding. Next, the sections were washed three times in 0.1M PBS and incubated overnight at 4°C with appropriately diluted primary antibodies (5μg/μL; Santa Cruz Biotech; sc-10790, sc-507, sc-316, sc-504). The next day, the sections were washed 3 times with 0.1M PBS Buffer followed immediately by incubation in appropriately diluted, according to the manufacturer, fluoro-tagged secondary antibody (Santa Cruz Biotech; sc-2784) for 45min at RT. Thereafter, the sections were washed

2 times with 0.1M PBS, stained with Sytox Green for 5min (1:5000 in 0.1M PBS; Invitrogen; s7020), washed 1 time with 0.1M PBS, mounted with aqueous mounting medium (Ultracruz Mounting Medium, sc-24941; Santa Cruz Biotech), and examined with appropriate filters under a confocal microscope (Car Zeiss Inc.).

Quantitative Proteomics

Whole protein was extracted from cervical tissue at 0h and 48h postpartum (n= 3) as described earlier under Western blot analysis. The supernatant was then immediately stored at -80°C and later transported to the core facility Laboratory of the David Murdock Research Institute under dry ice for proteomics analysis.

Sample Preparation: The samples were assayed using the Thermo Scientific Micro BCA Protein Assay kit to determine protein concentration. The samples were diluted to fall within the linear working range of the kit (5-200µg/mL), and the concentrations were calculated based on absorbance values compared to a BSA standard curve. The samples were filtered using a 3kD ultra centrifugal filter to exchange the dissolution solvent with a mass spectrometry friendly buffer. The sample (100µL) was diluted to 500µL with 50mM ammonium bicarbonate and filtered. The samples were rinsed with 200µL ammonium bicarbonate and filtered. The tubes were inverted and centrifuged to collect the sample.

A volume of each sample corresponding to 35µg of protein (based on the protein quantization results) was used. The sample volumes were made equal by adding 50mM ammonium bicarbonate (AmBic) to a volume of 29.8µL. A 1% solution of Rapigest was added to each sample to denature the proteins, and the mixture was placed in a shaking heated mixer at 40°C for 10 minutes. Disulfide bonds were reduced by adding 200mM dithiothreitol (DTT) to each sample and heating the tubes to 80°C for 15 minutes. Free sulfur atoms were alkylated with 400mM Iodoacetamide (IA) by placing the tubes in the dark for 30 minutes at room

temperature. A tryptic digest was performed by adding 0.7µg Gold-Mass Spectrometry grade Trypsin to each tube and incubating overnight at 37°C. Alcohol dehydrogenase (ADH) digest from yeast was added to a final concentration of 50fmol/µg protein. The trypsin reaction was stopped, and the Rapigest was degraded with the addition of 10% TFA/20% acetonitrile/70% water that was then heated to 60°C for 2 hours. The samples were centrifuged and the supernatant pipetted into auto sampler vials.

A protein standard (BSA) was carried through the reduction/alkylation and digestion steps and used as a QC of the sample preparation steps and instrument performance. LC solvents for peptide separation included **a**) water containing 0.1% formic acid; and **b**) acetonitrile containing 0.1% formic acid. The study sequence consisted of the study sample injections bracketed by a pair of QC injections. Data from all study samples were acquired using Data Dependent™ scans (Nth order double play) on the LTQ Orbit rap XL. Database searches were performed in Elucidator (Rosetta Bio software) using MASCOT (Matrix Sciences, London, UK). Analytical results were also viewed in Scaffold (Proteome Software, Portland, OR). QC and study samples were evaluated to confirm data quality. Liquid chromatography total ion current (TIC) outputs were assessed for signal quality and changes in signal intensity. Results were also monitored for signal trends, such as a consistent increase or decrease in TIC maximum values, and MASCOT search results were used to monitor the quality of the MS data.

Statistical Analysis

Western blot and real time PCR: Data for Western blot and real time PCR analyses were analyzed using Student's *t* test and ANOVA, followed by Scheffe's *F*-test for multiple comparisons. *P*-values of < 0.05 were considered to be statistically significant.

Proteomics: Raw MS data files for the study samples, collected on the Thermo Orbit rap XL system, were processed in Elucidator. MS data were grouped in Elucidator based on sample

group and aligned. Sample groups were used to assist in data alignment, feature identification, and were utilized for QC assessment and group comparisons. Data were processed from retention time, 8-90 min. Thermo Orbit rap data files were searched using the Mascot search engine against the SwissProt mouse database (appended with yeast ADH, March 02, 2010). The aligned mass features were annotated with these database search results using the results from the system Peptide Tellers and a predicted error rate of 1%. MS data were summarized to the feature level, normalized, and an error-weighted ANOVA test was performed to compare the expression results between sample groups. Candidate differentially expressed markers were determined based on a $p<0.01$. Features were summarized by protein based on the results of the database search.

Results

Morphological Changes in the Murine Cervix Postpartum

SEM analysis of cervices obtained from mice at 0h, 24h, and 48h postpartum (PP) displayed distinct morphological features at the time points (Fig 1). At 0h, the cervical epithelium displayed folds (Fig 1A-B) and micro-folds (Fig 1C-D), as well as less prominent epithelial cell borders, compared to both 24 and 48h PP. A layer of unidentified extracellular matrix or cell debris appeared at 24h PP (Fig 1 G-H) and was absent by 48h PP. At both 24h and 48h PP, the presence of "pits" or gaps in the cervical epithelium was observed, and the cell-cell borders were more pronounced than at 0h (Fig 1F-G, J-K). In order to further characterize the morphological changes of the postpartum cervix, we performed hematoxylin and eosin (H&E) staining. H&E stains revealed folded nature of the cervical epithelium at 0h PP (Fig 2A). At 24h PP a layer of unidentified cellular debris reported earlier under SEM data was observed (Fig 2D), but not seen at 48h PP (Fig 2G), consistent with the SEM findings.

Gene Expression in the Murine Cervix Postpartum

VEGF gene expression displayed a 13-fold increase at 0h PP compared to non-pregnant animals, with decreased expression at 48h PP relative to 0h PP, but elevated compared to non-pregnant (Fig 3A). HIF-1α displayed a similar expression pattern, with an 11-fold increase at 0h PP compared to a non-pregnant state, followed by a significant decrease in expression by 48h PP relative to 0h PP, and only slightly elevated compared to non-pregnant (Fig 3B). Both Flt-1 and KDR relative gene expression were elevated at 0h PP, with approximately 17-fold and 9-

fold increases, respectively, and expression declined significantly at 48h PP to a non-pregnant levels (Fig 3C-D).

Western Blot Analysis of Murine Postpartum Cervical Tissue

VEGF protein expression was found to be at the highest level at 0h PP, with levels decreasing approximately 2 fold by 16h PP, followed by slight decrease for the remaining time intervals (Figure 4A). The VEGFR, Flt-1, was found to be at its highest expression at 8h PP with levels decreasing in the remainder of time intervals, save for a slight increase at 24h PP relative to 16h PP (Figure 4D). It should be noted that the fold change from the highest expression, 8h PP, to the lowest expression, 48h, was less than half. In contrast, the other VEGFR, KDR, was found to increase steadily during the postpartum time intervals; with levels being lowest at 0h and leveling off at 40-48h PP (Figure 4C). HIF-1α protein expression pattern was similar to VEGF, i.e. it was elevated at 0h PP, and lowest at 48h PP (Figure 4B); however, there was an increase in expression from 16h to 24h PP, remaining elevated at 32h, and falling off again by 40h PP (Figure 4B).

Confocal Immunofluorescence Analysis of Murine Postpartum Cervical Tissue

The highest levels of VEGF were observed at 0h PP (Fig 5A), with the lowest levels occurring at 48h PP (Fig 5G). The most pronounced expressions were localized on the apical side of the epithelium, regardless of time interval. It is noteworthy that expression of VEGF was readily detected in the unidentified layer of cell debris observed at 24h PP (Fig 5D) and 32 h PP (Fig 5E). HIF-1α expression mirrored that of VEGF, i.e. with the highest levels at 0h PP (Fig 6A), lowest expression at 48h PP (Fig 6G), with expression preferentially localized at the apical side of the cervical epithelium at each time interval. Also, HIF-1α expression was similar to VEGF in that it was also readily expressed in the layer of cell debris at 24h PP (Fig 6D) and 32h PP (Fig

6E). The VEGF receptors, Flt-1 and KDR, demonstrate different patterns of expression postpartum. Flt-1 expression mirrored that of VEGF and HIF-1α with expression clearly highest at 0h PP (Fig 7A), lowest at 48h PP (Fig 7G), with expression localizing to the apical side of the epithelium and in the cell debris layer at both 24h PP (Fig 7D) and 32h PP (Fig 7E). Whereas, KDR expression seemed to be highest during the latter hours of postpartum (Fig 8D-F), but KDR was similar, with the strongest expression seen on the apical side of the epithelium, and was readily detected in the cell debris layer (Fig 8D-E).

Proteomics Analysis of Postpartum Murine Cervical Tissue

Proteomics analysis revealed several groups of proteins that were found to have significant changes between 0h and 48h PP (Fig 9). These proteins can be divided into 4 groups: 1) intermediate filaments (Fig 10), 2) actin-binding proteins (Fig 11), 3) immune-related proteins (Fig 12), and 4) hypoxia induced proteins (Fig 13).

Discussion

Of the four phases of cervical remodeling, postpartum repair is the least studied and to date, there is no study that has focused exclusively on this fourth and final phase of cervical remodeling. The present study is the first to do so and uses a variety of techniques to examine the morphological and molecular changes in the mouse cervix during the first 48h postpartum. The key findings presented here are: 1) Epithelial folds and cervical size are diminished during postpartum repair, 2) HIF-1α, VEGF, and Flt-1 expression are pronounced early in postpartum cervical repair, 3) KDR gene and protein expressions are variable, 4) Proteomics revealed variable expression of several intermediate filaments, cytoskeletal modulators, and proteins with immune- and/or wound healing properties.

Postpartum Morphology of the Cervix

The current SEM data shows the presence of cervical epithelial folds at 0h postpartum. These findings are consistent with our most recent work that utilized SEM and bromodeoxyuridine (BrdU) showing cervical epithelial proliferation leading up to parturition, as well as in non-pregnant ovariectomized mice that were treated with exogenous VEGF [14, 15]. Of interest, cervical tissue, as seen at low (50x) magnification, is clearly greater in size at 0h compared to 48h postpartum, which again, is consistent with cell proliferation leading up to parturition and postpartum recovery back to a non-pregnant state. The exact identity of the substance, appearing at 24h, covering the epithelial cells is unclear. It is possible that it could be derived from ECM, cervical mucus, or cellular debris. These observations and suggestions are consistent with previous reports that suggest postpartum repair may involve both clearance

and synthesis of ECM molecules [1], which may explain why in the present study, it (substance) was only seen at 24h postpartum but not at 0h and 48h postpartum. Through H&E, we were able to see changes within the cervical epithelium, mucosa, other intracellular structures, as well as the ECM. H&E also confirmed both the folded, convoluted nature of the cervical epithelium at 0h postpartum, as well as the covering substance at 24 h postpartum, revealed by SEM. The presence of cellular nuclei in the covering substance suggests that it could be cellular debris; however, it is also possible that there could be ECM molecules and/or cervical mucus in the covering substance.

Gene and Protein Expression Profiles of HIF-1α, VEGF, KDR, and Flt-1

We have previously characterized the expression profile of HIF-1α [in press] as well as VEGF and its receptors, KDR and Flt-1 [14, 15, 19] in pre-partum and 2 days postpartum. Here, we sought to determine their chronological expression profile postpartum at different time points between parturition and 48h postpartum in order to determine whether they have a temporal relationship with and, ultimately, have a role in postpartum cervical repair. Of interest, levels of HIF-1α, VEGF, and Flt-1 (gene and protein) were found to be elevated early postpartum and decreased to their lowest levels by 48h postpartum, a pattern that was similar to the genome-wide expression pattern of proteins associated with pro-inflammatory and wound healing revealed in our current proteomics analysis (see Quantitative Proteomics).

Due to the fact that HIF-1α is ultra-sensitive to changes in intracellular oxygen concentration, and is rapidly degraded under normoxic conditions [25] but activated and stabilized under hypoxic conditions [24, 25], HIF-1α's local tissue concentrations can be used to indirectly measure the local oxygen concentrations. Thus, elevated gene and protein expression of HIF-1α observed at 0h postpartum in the cervix in the present study suggests presence of a hypoxic state. Under such conditions (hypoxic), HIF-1α overall induces

transcription of a range of genes that promote angiogenesis and cell survival, notably VEGF, but also including metabolic enzymes, cytokines, growth factors, cytoskeletal proteins, and ECM molecules [24, 25]. Indeed, HIF-1α is the most potent inducer of VEGF [24], the key angiogenic molecule that is also known to be intricately linked to inflammation in a variety of tissue types, including the cervix [9, 14] and wound healing in general [13, 20-23].

Postpartum repair is characterized as a general inflammatory, wound healing process [1]. Specifically, there is a notable influx of tissue monocytes in the cervix shortly before birth as well as increased neutrophils postpartum [8]. These monocytes are subsequently activated and differentiate into M1 and M2 macrophages [1, 8]; however, the exact mechanisms that underlie the influx and activation of these immune cells during this process are unclear. It is possible that the local VEGF and HIF-1α surge reported here, and immediately prior to term [19], could be responsible for both the immune cell influx and activation for the following reasons: a) after injury the hypoxia-induced VEGF secretion establishes a gradient that mirrors the hypoxic gradient [22], and VEGF receptor-expression immune cells, including macrophages and neutrophils, respond chemotactically to VEGF, thus migrating to the injury/hypoxic site [13, 20, 23]; b) under hypoxic conditions, HIF-1α stimulates macrophages to secrete M1 pro-inflammatory cytokines [26]; and c) these recruited immune cells will secrete more VEGF and pro-inflammatory factors, as well as promote wound healing, angiogenesis, and VEGF production in keratinocytes and fibroblasts [20, 23], cells that are known to play a critical role in wound healing. Further studies are required to confirm this speculation and to shed more light on the alternate activation of the M2 phenotype.

While the pattern of HIF-1α, VEGF, and Flt-1 gene/protein expressions were in agreement, it is not so with KDR gene and protein expression. Real-time PCR demonstrated a decrease in mRNA expression of KDR between 0- and 48h postpartum; however, levels of KDR protein steadily increase, peaking between 40- and 48h postpartum, as revealed by both

western blot and confocal immunohistochemistry. It is likely that the turnover of KDR transcript is higher (more unstable) than protein. KDR is known to mediate most of VEGF's biological effects, including mitogenic, angiogenic, and cell survival properties [27], whereas, although Flt-1 does have a higher affinity for VEGF, it has weak tyrosine phosphorylation activity compared to KDR [28], and is of less functional significance. Further, the Flt-1 transcript can undergo alternative splicing that generates a soluble Flt-1 that acts to suppress the effects of VEGF [16, 28]. Flt-1 is also known to play a role in cell migration [28], and in certain cells that express Flt-1, such as blood platelets, macrophages, and neutrophils, it (Flt-1) mediates their chemotactic response to VEGF during wound healing [13, 23]. Based on these facts and taking into account their (VEGF receptors) differences in biochemical properties, it is likely that Flt-1 mediates VEGF processes associated with early hours of postpartum cervical repair, such as immune-related and wound healing functions, while KDR mediates the latter part of postpartum repair and VEGF, perhaps functions such as cell survival and angiogenesis. Collectively, these processes restore the cervix back to its non-pregnant state. Future functional studies are needed to test these speculations.

Quantitative Proteomics

Here, we identify over 150 proteins that were variably expressed, of which approximately 14 had a statistically significant change between 0- and 48h postpartum. Through an extensive literature search, these 14 proteins were placed into one or more of the following categories: a) intermediate filaments, b) actin binding proteins, c) hypoxia-induced proteins, and d) proteins involved in immune-modulation and/or wound healing.

The four intermediate filaments identified in the present study are keratins (type II 18 and type I 8), desmin, and vimentin; overall their expressions were elevated at 0hrs PP but dropped at 48hrs PP. Overall, intermediate filaments are among the three major cytoskeletal

systems in eukaryotic cells, which are known to supply cellular strength and integrity by acting as intracellular scaffolds [29]. The two keratins (type II 18 & type I 8) are paired together [30] and are the major keratins found in epithelium [31]. Desmin is associated with sarcomeres, nucleus, and mitochondria of all muscle types [32] and is known to maintain cell integrity during contractions, while helping force transmission and longitudinal load bearing [32, 33]. Generally, vimentin is accepted as the cytoskeletal element that maintains cell integrity [34] and offers resilience to cells undergoing high mechanical strain [35]; however, while the adult phenotypes in mice lacking keratin are obvious and severe, e.g. sever skin fragility [36], it is not so with vimentin. For instance, and of relevance to the current study, vimentin deficiency impairs wound healing both *in vitro* and *in vivo* by diminishing the mobility of fibroblasts and their ability to induce collagen contraction, which is essential in wound healing [37, 38]. Generally, wound healing in adulthood is characterized by an inflammatory response and by differentiation of the fibroblasts into a specialized contractile cell, the myofibroblast [39, 40]. It is feasible to speculate that the increased vimentin and desmin early in postpartum repair is necessary for the connective-tissue component of cervical repair, while keratin may play a similar role in the epithelial tissue [38].

Any cellular process involving movement, such as proliferation, migration, and morphological changes requires continuous and rapid reorganization (assembly, disassembly) of actin filaments [41]. Such processes (actin filament assembly, disassembly, and/or organization) are dependent on the presence of actin binding proteins. Here, we detected four actin binding proteins, whose expressions were elevated at 0h postpartum, but decreased by 48h postpartum. They include cytoplasmic gelsolin, filamin-A, the D isoform of plectin-1, and transgelin.

Gelsolin is a key regulator of actin filament disassembly, in a calcium dependent manner, and also promotes actin polymerization and reorganization by severing then

uncapping actin filaments [42]. Although mice lacking gelsolin are viable and fertile, they have deficiencies in the organization of actin-based domains in osteoclasts and in the migratory capacity of neutrophils and macrophages during inflammation and wound healing [43]. Also gelsolin deficiencies have been clinically associated with a variety of impairments in inflammation, cell invasion, immune cell recruitment, and wound healing [42-45].

Filamins are responsible for crosslinking actin filaments, anchoring trans-membrane proteins, and scaffolding proteins [46], whereas, Plectin is a very large protein found in nearly all mammalian cells that serves to link all three major components of the cytoskeleton to cellular junctions [47]. By holding the cytoskeleton together, plectin helps maintain cell integrity and elasticity [47]. Collectively, in the context of postpartum cervical repair, these actin-binding proteins could regulate a variety of locomotion-dependent processes, notably wound healing and immune responses. Further studies are needed to define their specific roles in the context of cervical repair.

Hypoxia is known to be involved in various physiological and/or pathological responses, but it may also play a role in parturition. For instance, in the high altitude mountain range of the Andes, expectant mothers will induce childbirth at term by climbing to high elevations with a lower oxygen environment or hypoxia. Similarly, it is likely that hypoxia could account for the increased risk of preterm labor associated with smoking. Interestingly, the current proteomics approach revealed two hypoxia-induced proteins, transgelin and vimentin, that were highly expressed at 0h postpartum. Transgelin is an actin-crosslinking protein known to be expressed in fibroblasts and smooth muscle [48, 49] and is strongly expressed in both the uterus and the cervix. Recent studies by Kim et al. (2012) demonstrated that transgelin is up regulated by hypoxia, independent of HIF-1α, and that it (transgelin) also activates the insulin-like growth factor receptor 1 [IGFR1] signaling pathway under hypoxic stress. The IGFR1 pathway has recently been shown to promote cell survival under hypoxic

stress [49, 50] by up regulation of HIF-1α gene transcription [50] and stabilization of HIF-1α protein [51]. This up regulation and stabilization of HIF-1α by the IGFR1 axis has been shown to induce VEGF expression during embryonic vasculogenesis [51] and angiogenesis in malignant tumor cells under hypoxic stress [50]. Whether transgelin acts upstream of HIF-1α and VEGF in postpartum cervical repair is, for now, speculative. The exact and diverse roles of trangelin during postpartum cervical repair require further inquiry. Like transgelin, vimentin has also been associated with hypoxia. For instance, it has been shown to redistribute among the endothelial cell into stable structures in response to hypoxia [52], is involved in general wound healing [53], and is known to play a role in migrating cells including fibroblasts, macrophages, endothelial cells, and invasive cancer cells [52-55]. Future studies are needed to examine the roles of these hypoxia-induced proteins in the postpartum phase of CR.

Postpartum repair has been previously characterized as a proinflammatory and wound healing process [3, 6, 7]. Our current proteomics data of postpartum cervical tissue are consistent with the earlier studies. Here, we identified several proteins that have known immune-related functions, notably glutamine gamma-glutamyltranferase 2 (often referred to as transglutaminase 2), gelsolin, lymphocyte antigen 6D, macrophage migration inhibitory factor [MIF], annexin A1, and phospholipase 2. Transglutaminases are ubiquitous enzymes that are important in posttranslational modification of proteins [56] that participate in coagulation and wound healing responses [57, 58]. Transglutaminase 2, is known to be an enzyme that is important in remodeling of the ECM [56] and, in this study, was found to be highly expressed at 0h postpartum followed by a decrease in expression at 48h postpartum. It is feasible that it may regulate cervical hemorrhage during parturition in addition to the extensive ECM remodeling that takes place after parturition [1, 3, 7]. The role of gelsolin in inflammation, immune responses, and wound healing has been discussed previously [42-45] and is consistent with previous studies that report increases in various immune cell populations just after birth

[8]. The other protein of interest detected at high levels at 0h postpartum compared to 48h postpartum was lymphocyte antigen 6D [LY6D]. LY6D is a marker found on mature B cells and specific populations of dendritic cells [59] and is implicated in DNA damage control [60], implying an increase in either dendritic or B cells postpartum; however, such cell types have not yet been reported postpartum.

The next protein involved in the immune response is macrophage migration inhibitory factor [MIF]. It was one of the earliest cytokines discovered in the 1960's. MIF is a pro-inflammatory cytokine involved in the innate immune response [61, 62] and was first characterized as playing a large role in delayed hypersensitivity reactions [63]. These reactions involve interactions between T cells and macrophages rather than antibodies, and MIF is an important cytokine, modulating the T cell responses [64] and T cell-macrophage interactions [65]. MIF is also known to be secreted by the pituitary [65], and further studies are needed to examine if parturition could be sufficient to induce pituitary MIF. With MIF being elevated at 48h postpartum, we speculate that a delayed hypersensitivity reaction could be taking place in the postpartum cervix, providing further support of the protection from microbial invasion explanation of the pro-inflammatory factors after birth.

One of the key changes happening during the postpartum phase of CR is the conversion of monocytes to activated macrophages (M1, classical proinflammatory, and M2, alternative anti-inflammatory) [1, 8]. The pro-inflammatory M1 and neutrophils would serve to aid with the clearance of ECM molecules [1] while protecting the birth canal from foreign invaders [7, 8]; whereas the anti-inflammatory effects could serve to keep the pro-inflammatory effects in balance [1], which if left unchecked could potential cause damage to the birth canal, putting subsequent pregnancies in jeopardy. In this study, we have identified a few potential players in the delicate balance of pro- and anti-inflammatory effects.

Lastly, two proteins associated with immune responses, annexin A1 and phospholipase A2, were elevated at 48h postpartum compared to 0h postpartum. These two proteins have contradictory effects. Phospholipase A2 is a calcium dependent enzyme that hydrolyzes glyercophospholipids into free intracellular arachidonic acid [66], the precursor for eicosanoids [67] including prostaglandins and leukotrienes, and, as such, is involved in inflammation and host defense [66]. In contrast, annexin A1, also known as lipocortin, is a calcium dependent phospholipid binding protein that will inhibit phospholipase A2 [68] as well as mediating VEGF-induced angiogenesis [69]. Glucocorticoids stimulate production of annexin A1 [68] and activation of M2 anti-inflammatory macrophages [70]. It is interesting that both of these are elevated simultaneously, i.e. at 48h postpartum, even though they have apparent contradictory effects. This pattern, however, supports earlier suggestions that there is a check and balance in play between pro- and anti-inflammatory factors in the postpartum repair of the cervix. From all the data gathered in the present study, along with what has already been characterized previously with regards to postpartum cervical repair, we propose a working model (Fig 14).

In summary, our data support the current thinking in the field of cervical remodeling, that postpartum repair involves a combination of pro- and anti-inflammatory actions. We also provide the first expression profile of VEGF, its receptors (Flt-1 & KDR), and HIF-1α and link their pattern of expression to hypoxia-related proteins revealed by proteomics. Future studies will assess the suitability of some of the key proteins identified in this study as potential markers for determining the phase of postpartum cervical repair.

References

1. Timmons BC, Akins M, Mahendroo M. Cervical remodeling during pregnancy and parturition. Trends Endocrinol Metabo 2010; 21:353-361.
2. Mahendroo M. Cervical remodeling in term and preterm birth: insights from an animal model. Reproduction 2012; 143: 429- 438.
3. Timmons BC, Mahendroo M. Process regulating cervical ripening differ from cervical dilation and postpartum repair: insights from gene expression studies. Reprod Sci 2007; 14:53-62.
4. Read CP, Word RA, Ruschenisky MA, Timmons BC, Mahendroo M. Cervical remodeling during pregnancy and parturition: molecular characterization of the softening phase in mice. Reprod 2007; 134:327-340.
5. Word RA, Li XH, Hnat M, Carrick K. Dynamics of cervical remodeling during pregnancy and parturition: mechanisms and current concepts. Semin Reprod Med 2007; 25: 69-79.
6. Bauer M, Mazza E, Jabareen M, Sultan L, Bajka M, Lang U, Zimmermann R, Holzapfel GA. Assessment of the in vivo biomechanical properties of the human uterine cervix in pregnancy using the aspiration test a feasibility study. Euro J OB/GYN Reprod Bio 2009; 144S:S77-S81.
7. Gonzalez JM, Xu H, Chai J, Ofori E, Elovitz MA. Preterm and term cervical ripening in CD1 mice (*Mus musculus*): similar or divergent molecular mechanisms? Biol Reprod 2009; 81: 1226-1232.
8. Timmons BC, Fairhurst AM, Mahendroo M: Temporal changes in myeloid cells in the cervix during pregnancy and parturition. Journal Immuno 2009; 182: 2700-2707.
9. Nguyen BT, Minkiewicz V, McCabe E, Cecile J, Mowa CN. Vascular endothelial growth factor induces mRNA expression of pro-inflammatory factors in the uterine cervix of mice. Biomed Res 2012; 33: 363-372.
10. Ferrara N. Vascular endothelial growth factor: basic science and clinical progress. Endocr Rev 2004; 25: 581-611.
11. Simons M. Integrative signaling in angiogenesis. Mol Cell Biochem 2004; 264: 99-102.
12. Eichmann A, Simons M. VEGF signaling inside vascular endothelial cells and beyond. Curr Opin Cell Biol 2012; 24: 188-193.
13. Eming SA, Krieg T. Molecular mechanisms of VEGF-A action during tissue repair. J Invest Dermatol 2006; 11: 79-86.
14. Mowa CN, Li T, Jesmin S, Folkesson HG, Usip SE, Papka RE, Hou G. Delineation of VEGF-regulated genes and functions in the cervix of pregnant rodents by DNA microarray analysis. Reprod Bio Endocrinol 2008; 6: 1-10.
15. Donnelly S, Nguyen BT, Rhyne S, Estes J, Jesmin S, Mowa CN. Vascular endothelial growth factor induces growth of the uterine cervix and immune cell recruitment in mice. J Endocrinol 2013; 217: 83-94.
16. Stuttfield E, Ballmer-Hofer K. Structure and function of VEGF receptors. *Life* 2009; 6: 915-922
17. Ladomery MR, Harper SJ, Bates DO. Alternative splicing in angiogenesis: The vascular endothelial growth factor paradigm. Cancer Letters 2007; 249: 133-142.

18. Harper SJ, Bates DO. VEGF-A splicing the key to anti-angiogenic therapeutics? Nat Rev Cancer 2008; 8: 880-887.
19. Mowa CN, Jesmin S, Sakuma I, Usip S, Togashi H, Yoshioka M, Hattori Y, Papka R. Characterization of vascular endothelial growth factor (VEGF) in the uterine cervix over pregnancy: effects of denervation and implications for cervical ripening. J Histochem Cytochem 2004; 52: 1665-1674.
20. Galiano RD, Tepper OM, Pelo CR, Bhatt KA, Callaghan M, Bastidas N, Bunting S, Steinmetz HG, and Gurtner GC. Topical vascular endothelial growth factor accelerates diabetic wound healing through increased angiogenesis and by mobilizing and recruiting bone marrow-derived cells. Am J Pathology 2004; 164: 1935-1947.
21. Mowa CN, Hoch R, Montavon CL, Jesmin S, Hindman G, Hou G. Estrogen enhances wound healing in the penis of rats. Biomed Res 2008; 29: 267-270
22. Alberts B, Johnson A, Lewis J, Raff M, Roberts K, Walter P. Molecular Biology of the Cell. New York: Garland Science; 2008: 1417-1482.
23. Bao P, Kodra A, Tomic-Canic M, Golinko MS, Ehrlich HP, Brem H. The role of vascular endothelial growth factor in wound healing. J Surgical Rese 2009; 15**:** 347-58.
24. Majmundar AJ, Wong WJ, Simon MC. Hypoxia inducible factors and the response to hypoxic stress. Mol Cell 2010; 40: 294-309.
25. Semenza GL. Hydroxylation of HIF-1: Oxygen sensing at the molecular level. Physiol 2004; 19: 176-182.
26. Acosta-Iborra B, Elorza A, Olazabal IM, Martin-Cofreces NB, Martin-Puig S, Miro M, Calzada MJ, Aragones J, Sanchez-Madrid F, Landazuri MO. Macrophage oxygen sensing modulates antigen presentation and phagocytic functions involving IFN-γ production through the HIF-1α transcription factor. J Immunol 2009; 182: 3155-3164.
27. Ge X, Zhao L, He L, Chen W, Li X. Vascular endothelial growth factor receptor 2 (VEGFR2, Flk-1/KDR) protects HEK293 cells against $CoCl_2$-induced hypoxic toxicity. Cell Biochem Funct 2012; 30: 151-157.
28. Roskoski R Jr. Vascular endothelial growth factor (VEGF) signaling in tumor progression. Crit Rev Oncol Hematol 2007; 62: 179-213.
29. Fuchs E. Intermediate filaments and disease: mutations that cripple cell strength. J Cell Biol 1994; 125: 511-516.
30. Singla A, Moons DS, Snider NT, Wagenmaker ER, Jayasundera VB, Omary MB. Oxidative stress, Nrf2 and keratin up-regulation associate with Mallory-Denk formation in mouse erythropoietic protoporphyra. Hepatology 2012; 56: 322-331.
31. Tao GZ, Looi KS, Toivola DM, Strnad P, Zhou Q, Liao J, Wei Y, Habtezion A, Omary MB. Keratins modulate the shape and function of hepatocyte mitochondria: a mechanism for protection from apoptosis. J Cell Sci 2009; 122: 3851-3855.
32. Paulin D, Li Z. Desmin: a major intermediate filament protein essential for structural integrity and function of muscle. Exp Cell Res 2004; 301: 1-7.
33. Bonakdar N, Luczak J, Lautscham L, Czonstke M, Koch TM, Mainka A, Jungbauer T, Goldmann WH, Schroder R, Fabry B. Biomechanical characterization of desminopathy in primary human myoblasts. Biochem Biophys Res Commun 2012; 419: 703-707.
34. Goldman RD, Khuon S, Chou YH, Opal P, Steinert PM. The function of intermediate filaments in cell shape and cytoskeletal integrity. J cell Biol 1996; 134: 971-983.
35. Haudenschild DR, Chen J, Pang N, Steklov N, Grogan SP, Lotz MK, D'Lima DD. Vimentin contributes to changes in chondrocyte stiffness in osteoarthritis. J Orthop Res 2011; 29: 20-25.
36. Lloyd C, Yu QC, Cheng J, Turksen K, Degenstein L, Hutton E, Fuchs E. The basal keratin network of stratified squamous epithelia: defining K15 function in the absence of K14. J Cell Biol 1995; 129: 1329-1344.

37. Eckes B, Dogic D, Colucci-Guyon E, Wang N, Maniotis A, Ingber D, Merckling A, Langa F, Aumailley M, Delouvee A, Koteliansky V, Babinet C, Kreig T. Impaired mechanical stability, migration and contractile capacity in vimentin-deficient fibroblasts. J Cell Sci 1998; 111: 1897-1907.
38. Eckes B, Colucci-Guyon E, Smola H, Nodder S, Babinet C, Krieg T, Martin P. Impaired wound healing in embryonic and adult mice lacking vimentin. J Cell Sci 2000; 113: 2455-2462.
39. Gabbiani G, Ryan GB, Majne G. Presence of modified fibroblasts in granulation tissue and their possible role in wound contraction. Experientia 1971; 27: 549-550.
40. Martin P. Wound healing-aiming for perfect skin regeneration. Science 1997; 276:75-81.
41. dos Remedios CG, Chhabra D, Kekic M, Dedova IV, Tsubakihara M, Berry DA, Nosworthy NJ. Actin binding proteins: regulation of cytoskeletal filaments. Physiol Rev 2003; 83: 433-473.
42. Sun HQ, Yamamoto M, Mejillano M, Yin HL. Gelsolin, a multifunctional actin regulatory protein. J Biol Chem 1999; 274: 33179-33182.
43. Witke W, Sharpe AH, Hartwig JH, Azuma T, Stossel TP, Kwiatkowski DJ. Hemostatic, inflammatory, and fibroblast responses are blunted in mice lacking gelsolin. Cell 1996; 81: 41-51.
44. Spinardi L, Witke W. Gelsolin and diseases. Subcell Biochem 2007; 45: 55-69.
45. Goncalves AF, Dias NG, Moransard M, Correia R, Pereira JA, Witke W, Suter U, Relvas JB. Gelsolin is required for macrophage recruitment during remyelination of the peripheral nervous system. Glia 2010; 58: 706-715.
46. Wang Q, Dai XQ, Li Q, Wang Z, Cantero Mdel R, Li S, Shen J, Tu JC, Cantiello H, Chen XZ. Structural interaction and functional regulation of polysystin-2 by filamin. PLoS One 2012; 7: e40448.
47. Wiche G. Role of plectin in cytoskeleton organization and dynamics. J Cell Sci 1998; 111: 2477-2486.
48. Kim TR, Moon JH, Lee HM, Cho EW, Paik SG, Kim IG. SM22alpha inhibits cell proliferation and protects against anticancer drugs and gamma-radiation in HepG2 cells: involvement of metallothioneins. FEBS Lett 2009; 583: 3356-3362.
49. Kim TR, Cho EW, Paik SG, Kim IG. Hypoxia-induced SM22α in A549 cells activates the IGF1R/PI3K/Akt pathway, conferring cellular resistance against chemo-and radiation therapy. FEBS Lett 2012; 586: 303-309.
50. Gariboldi MB, Ravizza R, Monti E. The IGFR1 inhibitor NVP-AEW541 disrupts a pro-survival and pro-angiogenic IGF-STAT3-HIF1 pathway in human glioblastoma cells. Biochem Pharmacol 2010; 80: 455-462.
51. Piecewicz SM, Pandey A, Roy B, Xiang SH, Zetter BR, Sengupta S. Insulin-like growth factors promote vasculogenesis in embryonic stem cells. PLoS ONE 2012; 7: e32191.
52. Lui T, Guevara OE, Warburton RR, Hill NS, Gaestel M, Kayyali US. Regulation of vimentin intermediate filaments in endothelial cells by hypoxia. Am J Physiol Cell Physiol 2010; 299: C363-373.
53. Rogel MR, Soni PN, Troken JR, Sitikov A, Trejo HE, Ridge KM. Vimentin is sufficient and required for wound repair and remodeling in alveolar epithelial cells. FASEB J 2011; 25: 3873-3883.
54. Hefland BT, Mendez MG, Murthy SN, Shumaker DK, Grin B, Mahammad S, Aebi U, Wedig T, Wu YI, Hahn KM, Inagaki M, Herrmann H, Goldman RD. Vimentin organization modulates the formation of lamellipodia. Mol Biol Cell 2011; 22: 1274-1289.
55. Glaser-Gabay L, Raiter A, Battler A, Hardy B. Endothelial cell surface vimentin binding peptide induces angiogenesis under hypoxic/ischemic conditions. Microvasc Res 2011; 82: 221-226.

56. Sabatino AD, Vanoli A, Giuffrida P, Luinetti O, Solcia E, Corazza GR. The function of tissue transglutaminase in celiac disease. Autoimmun Rev 2012; 11:746-753.
57. Aeschlimann D, Paulsson M. Transglutaminases: protein cross-linking enzymes in tissues and body fluids. Thromb Haemost 1994; 71: 402-415.
58. Upchurch HF, Conway E, Patterson MK Jr, Maxwell MD. Localization of cellular transglutaminases on the extracellular matrix after wounding: characteristics of the matrix bound enzyme. J Cell Physiol 1991; 149: 375-382.
59. Inlay MA, Bhattacharya D, Sahoo D, Serwold T, Seita J, Karsunky H, Plevritis SK, Dill DL, Weissman IL. Ly6d marks the earliest stage of B-cell specification and identifies the branchpoint between B-cell and T-cell development. Gene Dev 2009; 23: 2376-2381.
60. Kurosawa M, Jeyasekharan AD, Surmann EM, Hashimoto N, Venkatraman V, Kurosawa G, Furukawa K, Venkitaraman AR, Kurosawa Y. Expression of LY6D is induced at the surface of MCF10A cells by X-ray irradiation. FEBS J 2012; 279: 4479-4491.
61. Calandra T. Macrophage migration inhibitory factor and host innate immune responses to microbes. Scand J Infect Dis 2003; 35: 573-576.
62. Roger T, Delaloye J, Chanson AL, Giddey M, Le Roy D, Calandra T. Macrophage migration inhibitory factor deficiency is associated with impaired killing of gram-negative bacteria by macrophages and increased susceptibility to Klebsiella pneumonia sepsis. J Infect Dis 2013; 207: 331-339.
63. Bloom BR, Bennett B. Relation of the migration inhibitory factor (MIF) to delayed-type hypersensitivity reactions. Ann NY Acad Sci 1970; 169: 258-265.
64. Choi S, Kim HR, Leng L, Kang I, Jorgensen WL, Cho CS, Bucala R, Kim WU. Role of macrophage inhibitory factor in the regulatory T cell response of tumor-bearing mice. J Immunol 2012; 189: 3905-3913.
65. Nishihira J. Macrophage migration inhibitory factor (MIF): it's essential role in the immune system and cell growth. J Interferon Cytokine Res 2000; 20: 751-762.
66. Murakami M, Kudo I. Phospholipase A2. J Biochem 2002; 131: 285-292.
67. Dennis EA. Diversity of group types, regulation, and function of phospholipase A2. J Biol Chem 1994; 269: 13057-13060.
68. Gavins FN, Hickey MJ. Annexin A1 and the regulation of innate and adaptive immunity. Front Immunol 2012; 3: doi: 10.3389/fimmu.2012.00354 Epub 2012 Nov 27.
69. Pin AL, Houle F, Fournier P, Guillonneau M, Paquet ER, Simard MJ, Royal I, Huot J. Annexin A1-mediated endothelial cell migration and angiogenesis are regulated by vascular endothelial growth factor (VEGF)-induced inhibition of miR-196a expression. J Biol Chem 2012; 287: 30541-30551.
70. Mantovani A, Sica A, Locati M. New vistas on macrophage differentiation and activation. Euro J Immunol 2006; 37: 14-16.

Figures

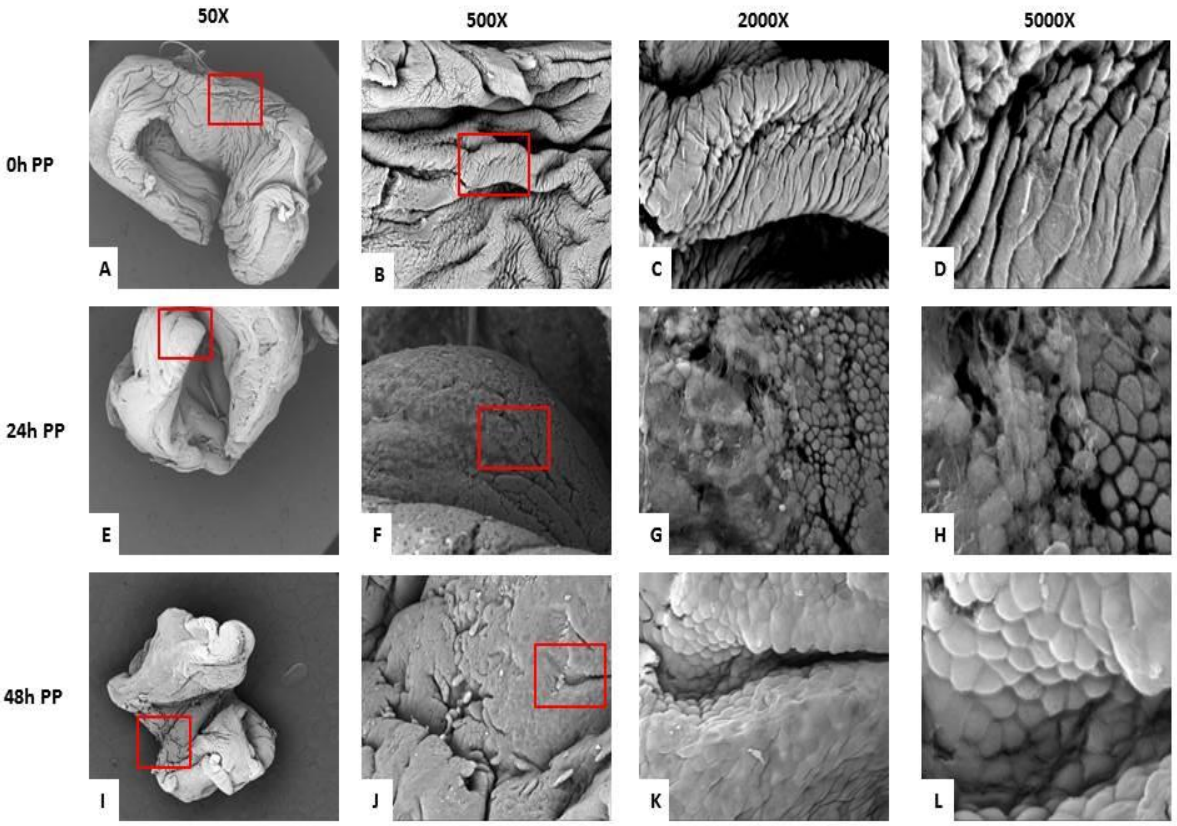

Figure 1: Scanning electron microscopy (SEM) of postpartum murine cervical tissue. Under low magnification (50X) decrease in size was obvious from 0h to 48h postpartum (PP). Cervical epithelial folds, as well as diminished cell-cell borders were prominent at 0h PP at higher magnifications (500X-5,000X). An unidentified "covering" was observed at 24h PP (2000X-5000X), but was absent at both 0h and 48h PP.

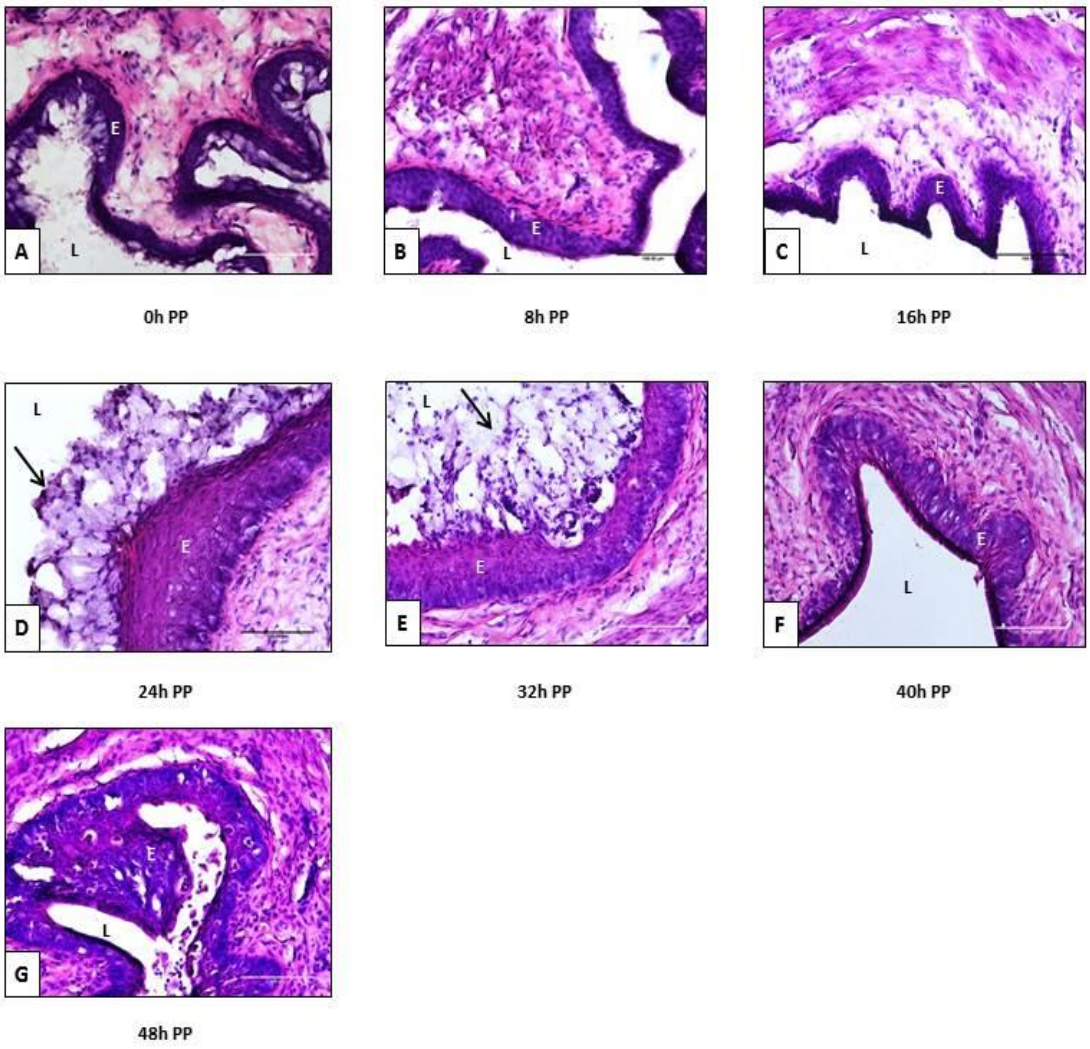

Figure 2: H&E staining of postpartum murine cervical tissue. During the hours after parturition (0h postpartum (PP)) the cervical tissue appeared edematous the first 24h PP but disappeared thereafter. At 24 and 32h PP a layer of unidentified cellular debris (indicated by arrows) was observed. **E** denotes cervical epithelium, **L** denotes cervical lumen. All images were taken at 20X.

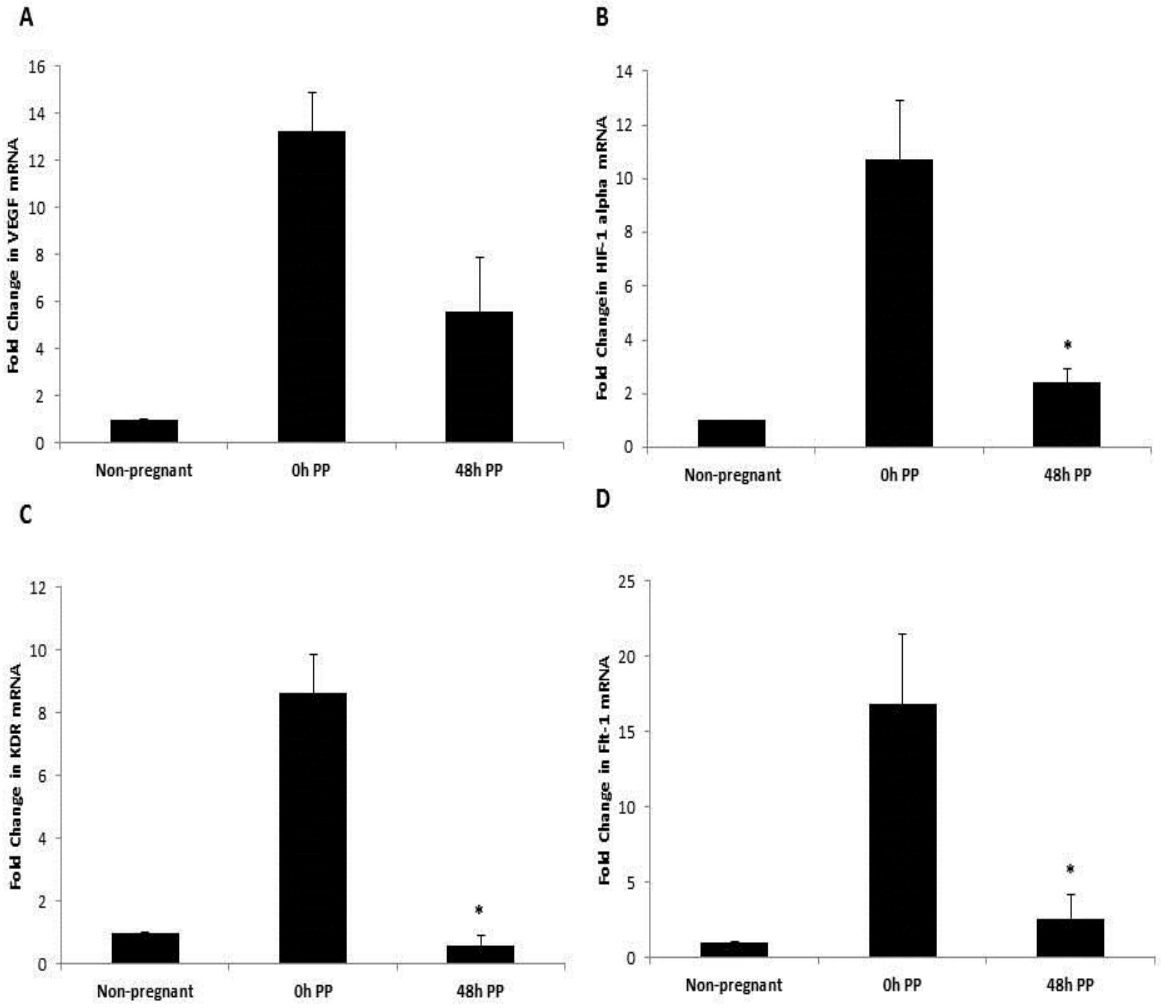

Figure 3: Real-time PCR analysis of select genes in the postpartum murine cervix. All genes of interest were found to be highly expressed at 0h PP, decreasing significantly by 48h PP for B) HIF-1α (p value 0.02), C) KDR (p value 0.008), and D) Flt-1 (p value 0.04) relative to 0h. A) VEGF expression decreased at 48h PP but was not found to be significant and is several fold above the control, non-pregnant animals.

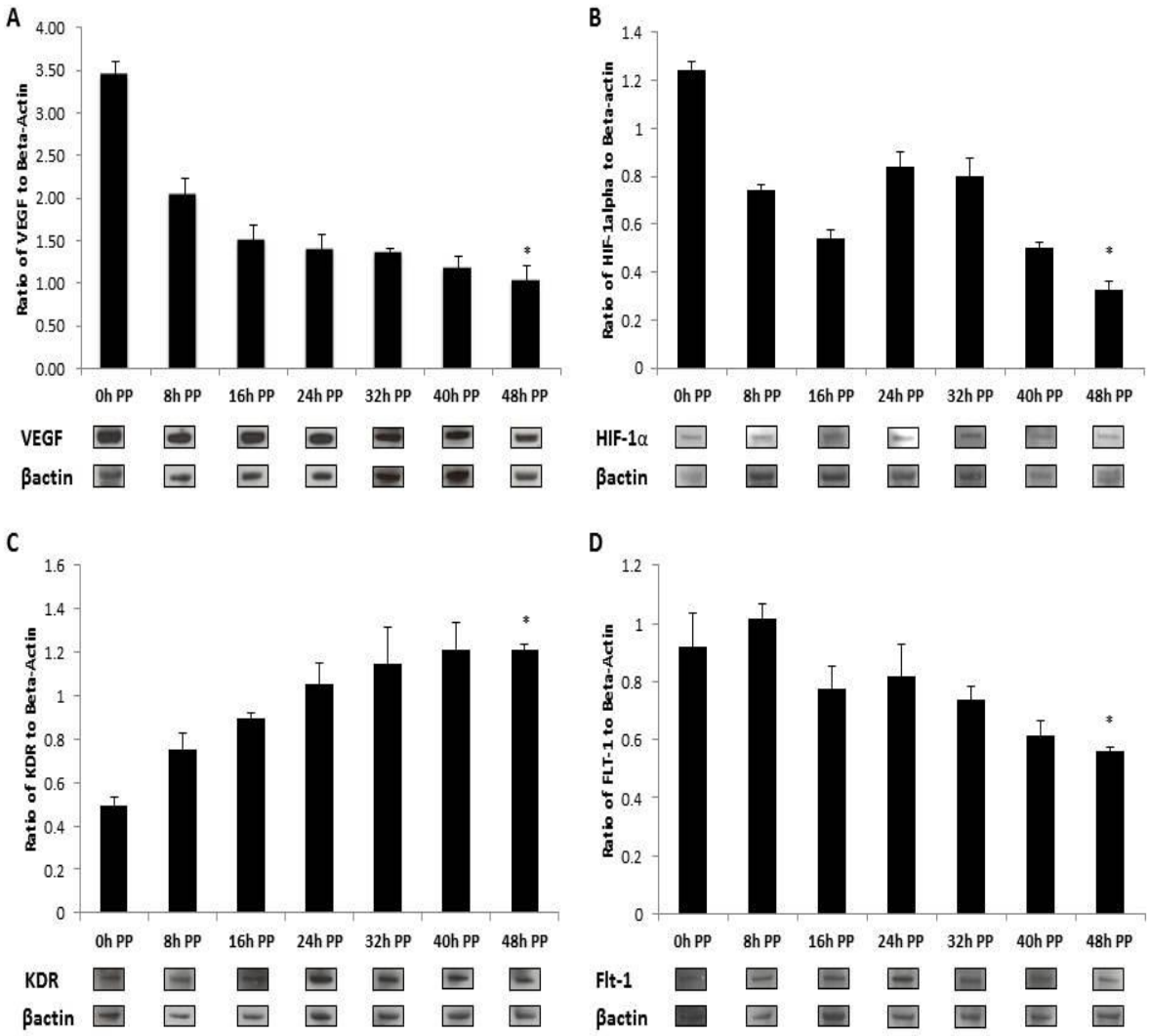

Figure 4: Western blot analysis of select proteins in the postpartum murine cervix. A) VEGF protein expression relative to βactin, (*) shows statistical significance between 0h and 48h PP (p value = 4.56×10^{-8}); B) HIF-1α protein expression relative to βactin, (*) shows statistical significance between 0h and 48h PP (p value = 3.08×10^{-8}); C) KDR protein expression relative to βactin, (*) shows statistical significance between 0h and 48h PP (p value = 0.0005); and D) Flt-1 protein expression relative to βactin, (*) shows statistical significance between 0h and 48h PP (p value = 0.008).

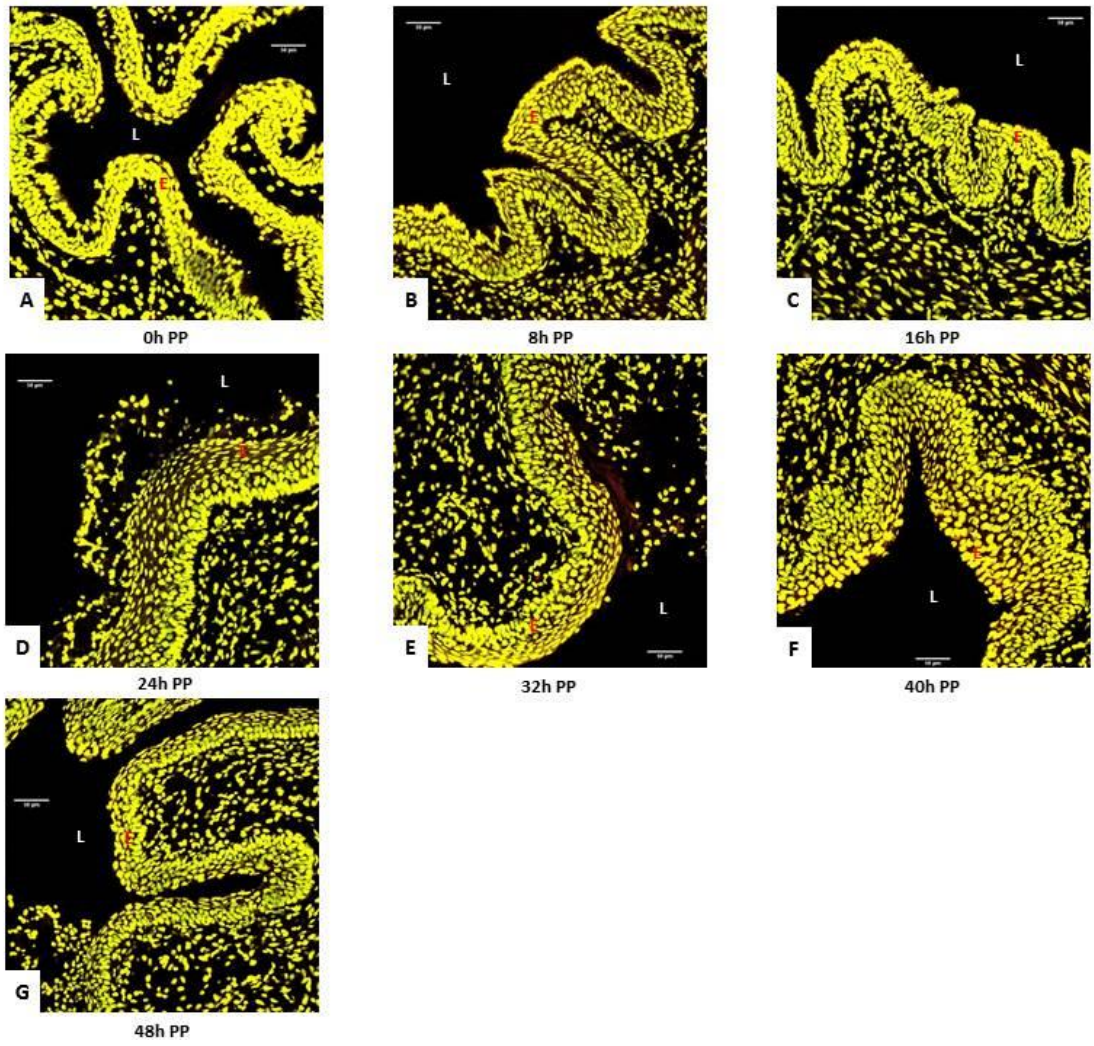

Figure 5: VEGF expression in the postpartum murine cervix as revealed by confocal immunofluorescence. VEGF stained with Texas red antibodies, nuclei stained with Sytox green, and any overlap between the two is seen as yellow. **E** denotes the epithelium and **L** denotes the lumen.

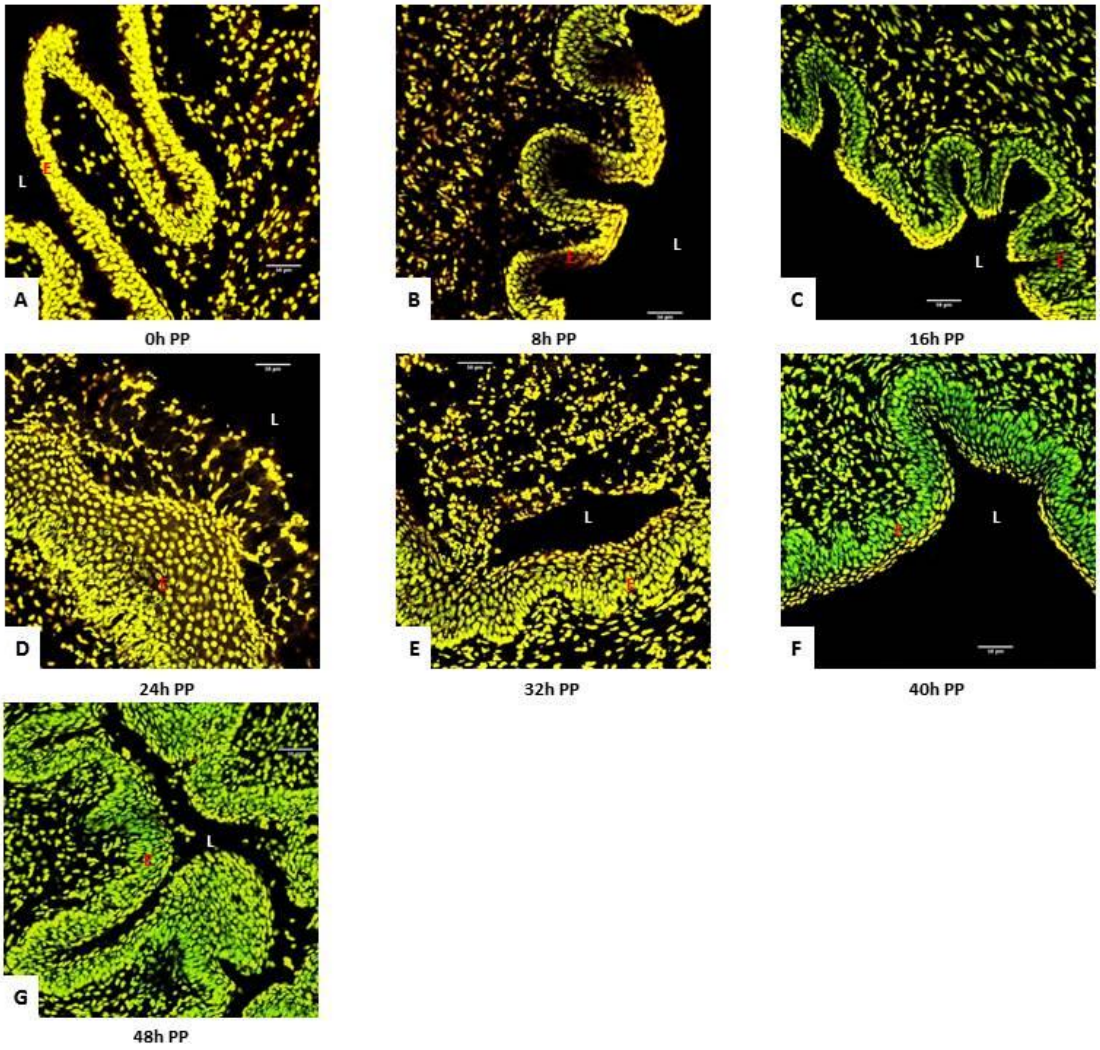

Figure 6: HIF-1α expression in the postpartum murine cervix as revealed by confocal immunofluorescence. HIF-1α stained with Texas red antibodies, nuclei stained with Sytox green, and any overlap between the two is seen as yellow. **E** denotes the epithelium and **L** denotes the lumen.

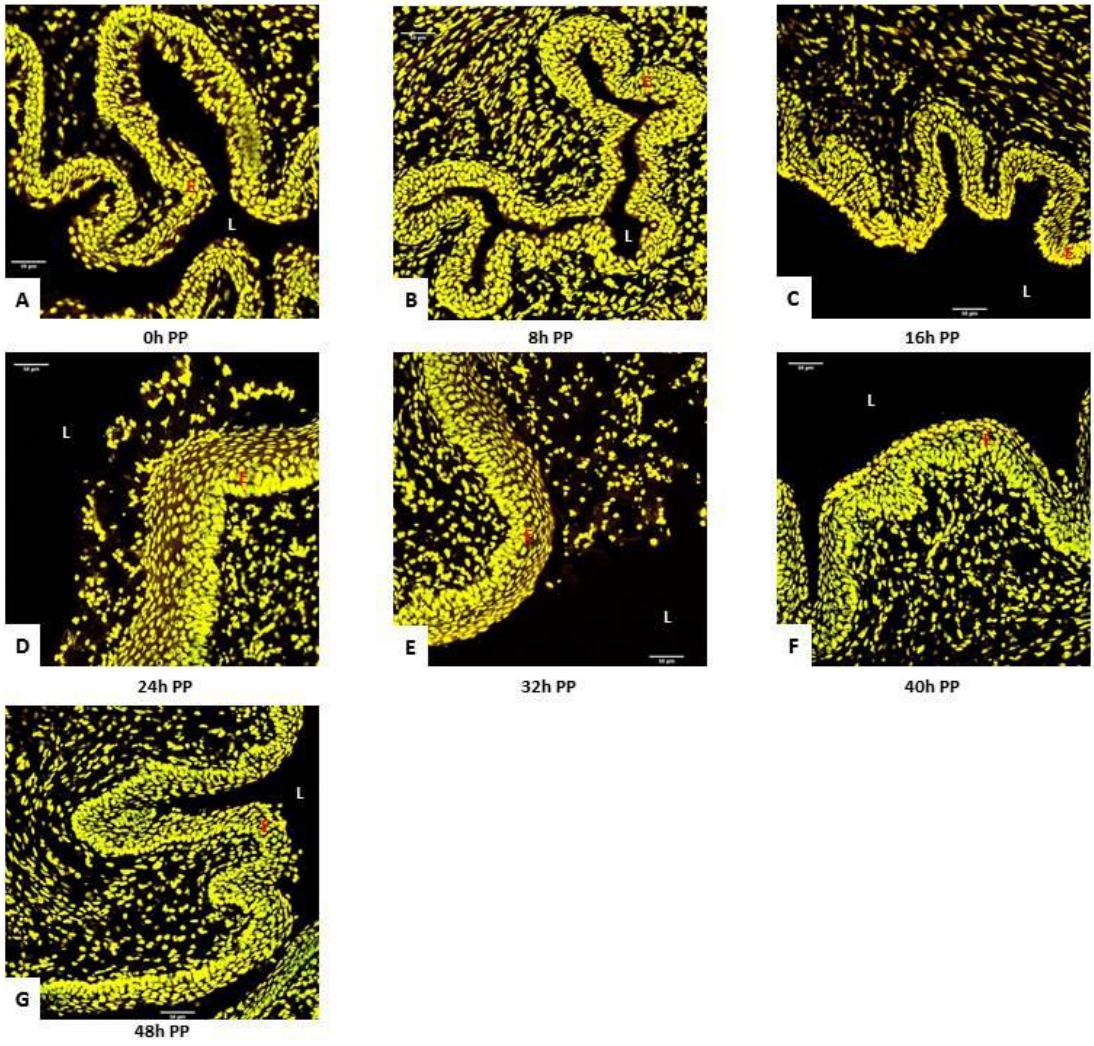

Figure 7: Flt-1 expression in the postpartum murine cervix as revealed by confocal immunofluorescence. Flt-1 stained with Texas red antibodies, nuclei stained with Sytox green, and any overlap between the two is seen as yellow. **E** denotes the epithelium and **L** denotes the lumen.

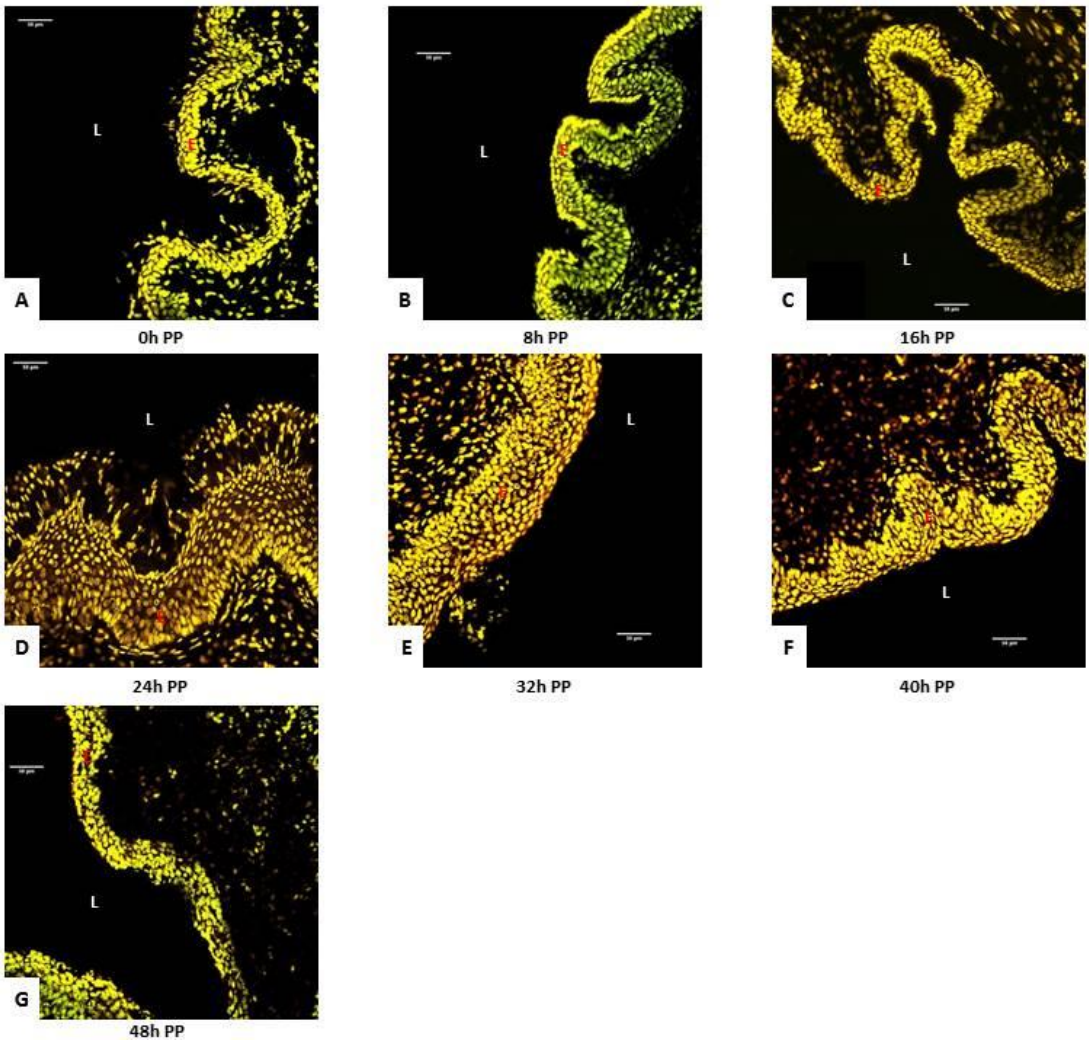

Figure 8: KDR expression in the postpartum murine cervix as revealed by confocal immunofluorescence. KDR stained with Texas red antibodies, nuclei stained with Sytox green, and any overlap between the two is seen as yellow. **E** denotes the epithelium and **L** denotes the lumen.

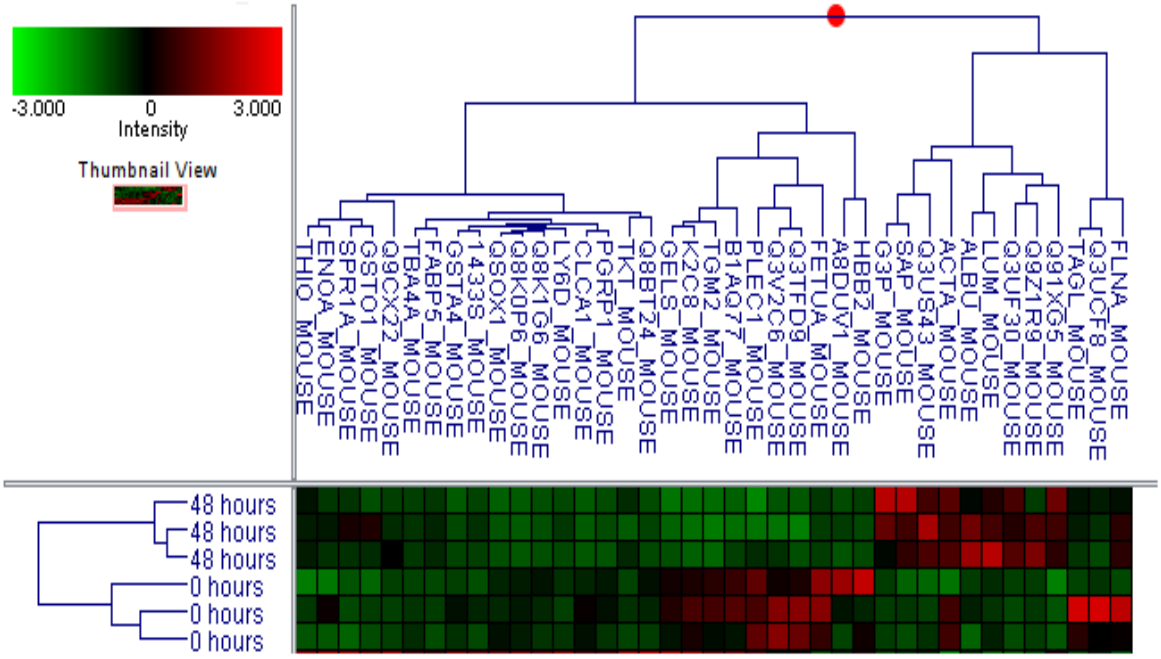

Figure 9: Quantitative proteomics analysis of protein expression in the postpartum murine cervix. Over 150 proteins were identified, with a small subset demonstrating statistically significant changes postpartum. Red indicates higher intensity, and green indicates lower intensity.

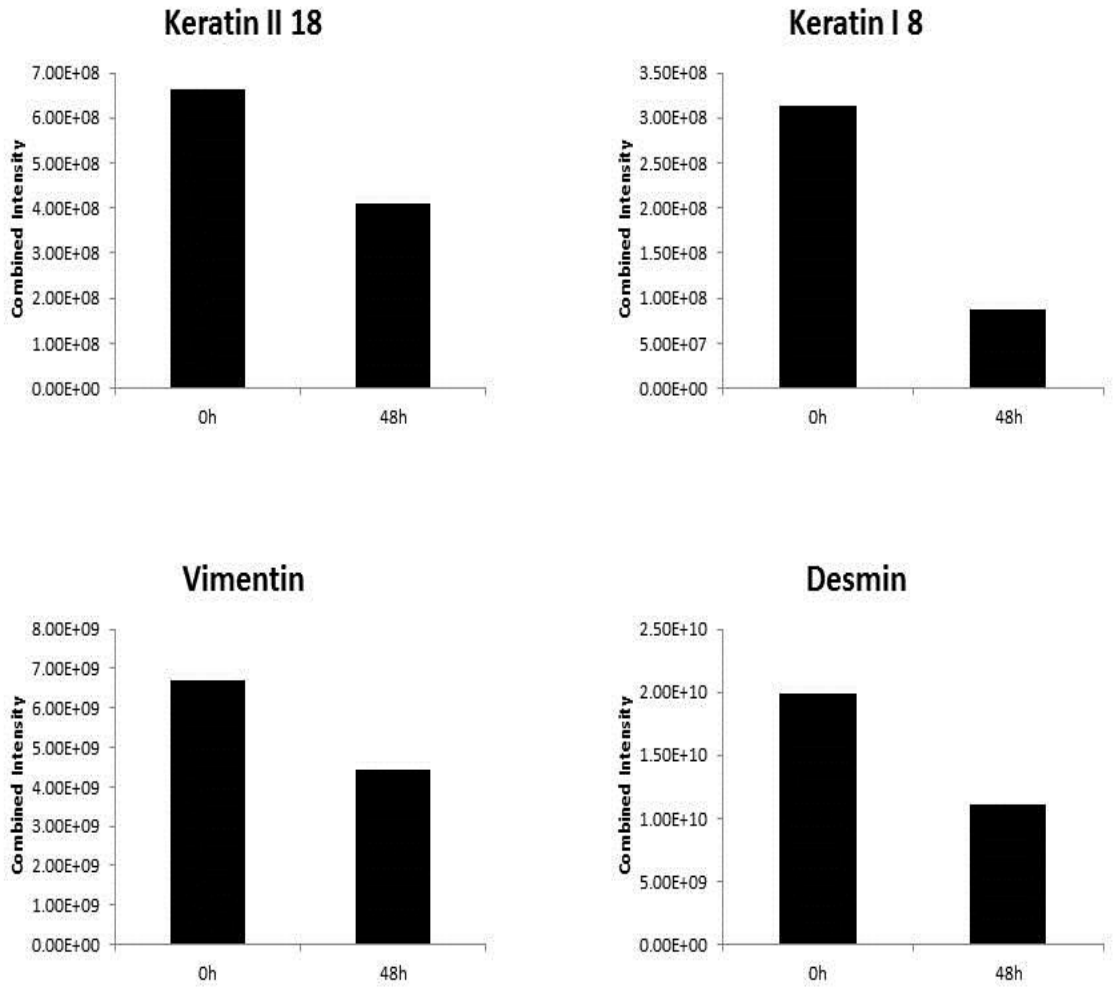

Figure 10: Quantitative proteomics expression analysis of intermediate filament proteins in the postpartum murine cervix. Four intermediate filaments: keratin type II 18, keratin type I 8, vimentin, and desmin were identified to have variable expression in the cervix postpartum, and a clear expression pattern was visible: elevated at 0h PP and decreased at 48h PP.

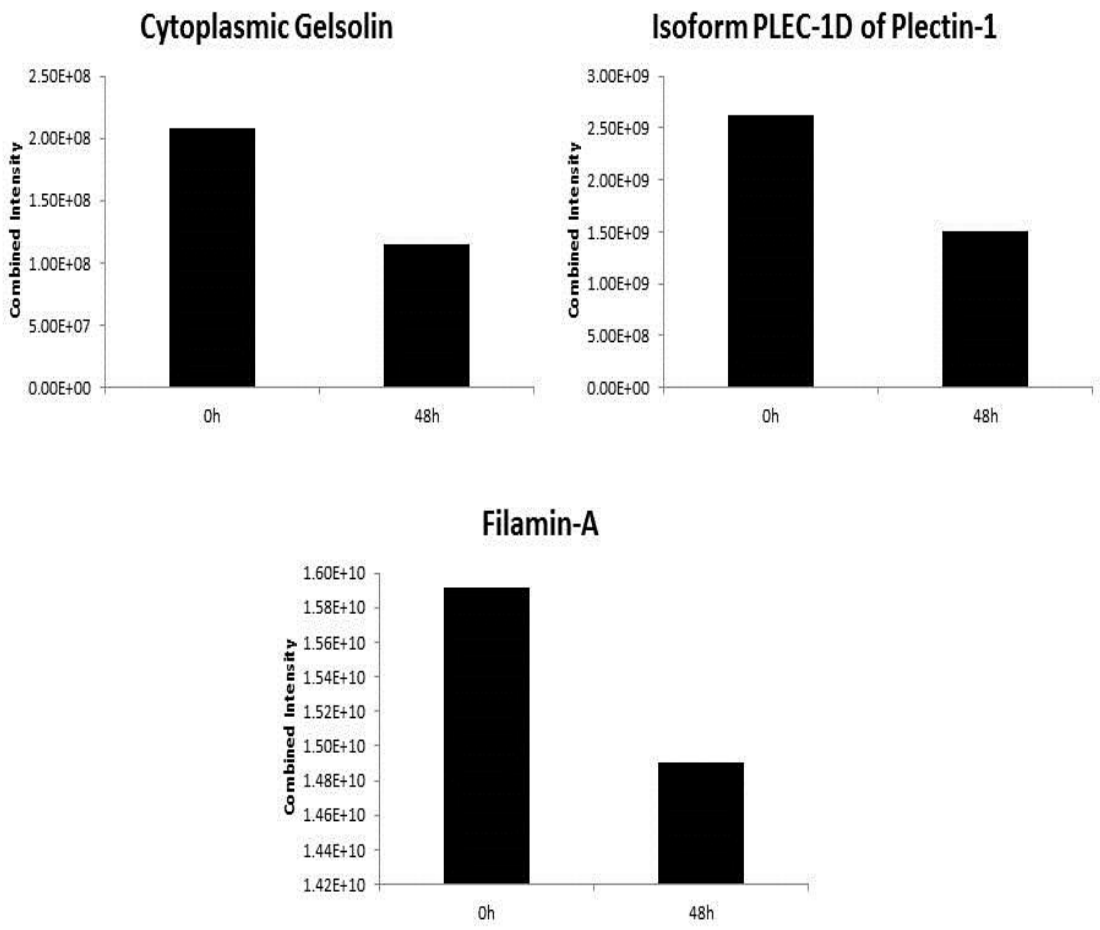

Figure 11: Quantitative proteomics expression analysis of actin-binding proteins in the postpartum murine cervix. Three actin-binding proteins: gelsolin, plectin-1, and filamin-A were identified to have variable expression in the postpartum cervix, and an expression pattern was apparent: elevated at 0h PP and decreased at 48h PP.

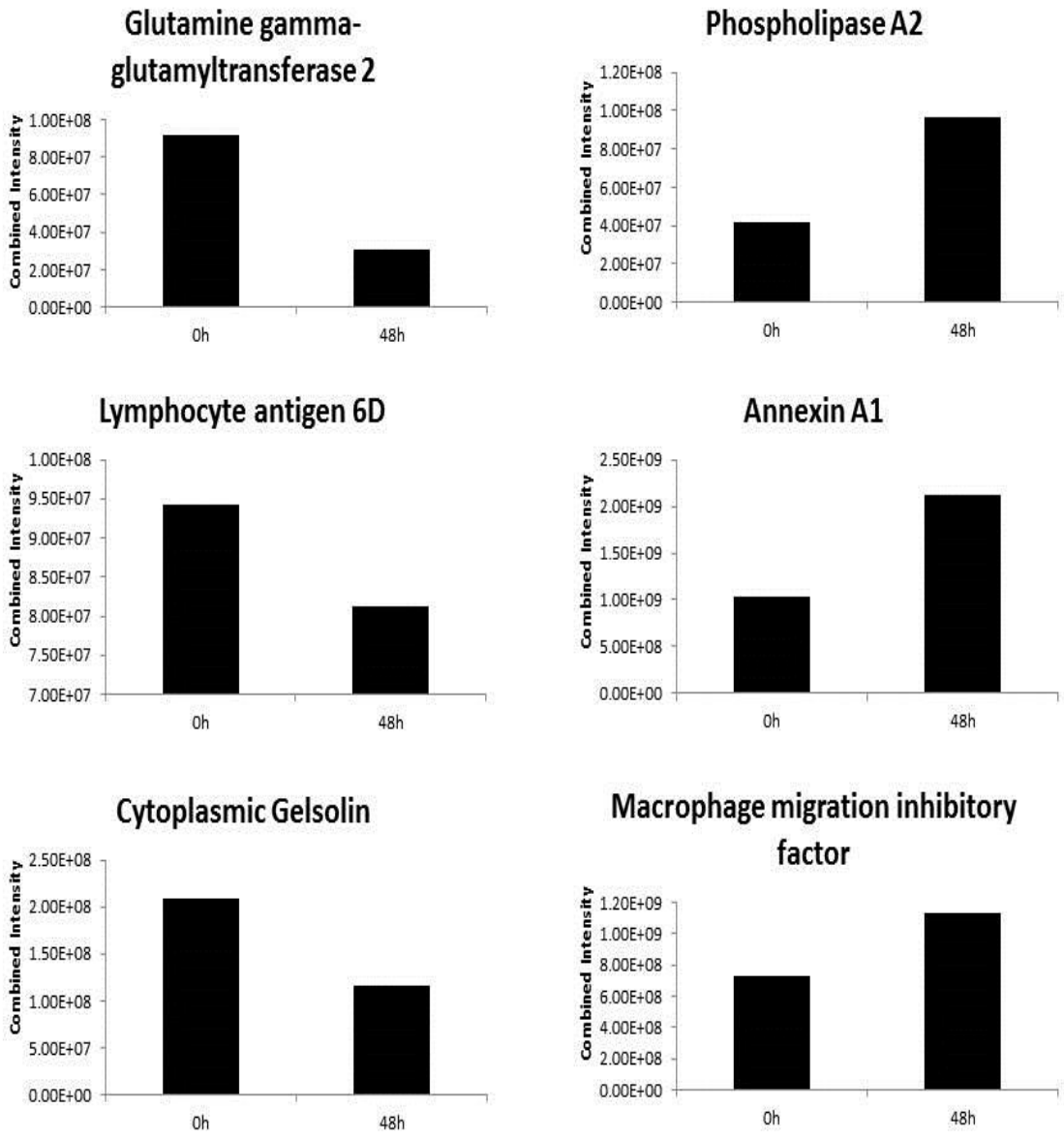

Figure 12: Quantitative proteomics expression analysis of proteins that are involved in immune-modulation and wound healing in the postpartum murine cervix. Six proteins that are known to have immune-related or wound healing functions were found to have variable expression in the postpartum cervix, and the expression pattern is variable: some elevated at 0h others 48h PP.

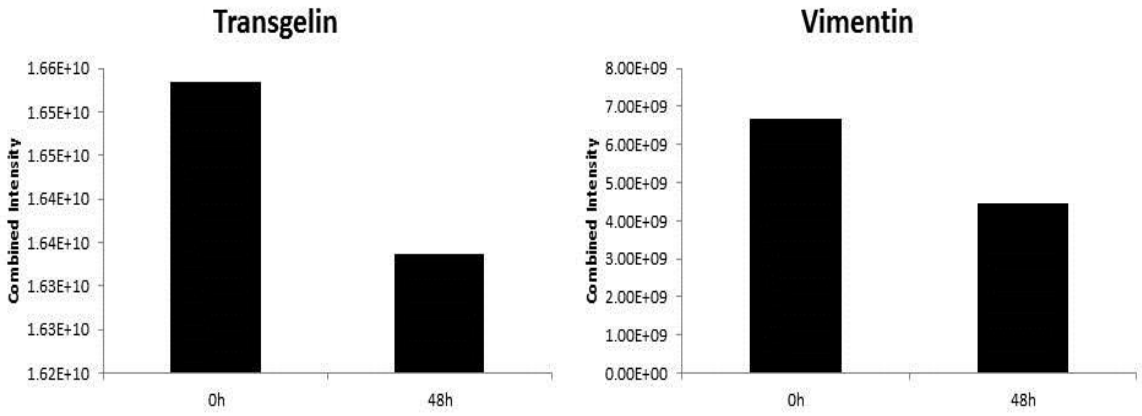

Figure 13: Quantitative proteomics expression analysis of proteins regulated by hypoxia in the postpartum murine cervix. Two hypoxia induced proteins: transgelin and vimentin were identified to have variable expression in the postpartum cervix, and an expression pattern is apparent: elevated at 0h PP and decreased at 48h PP.

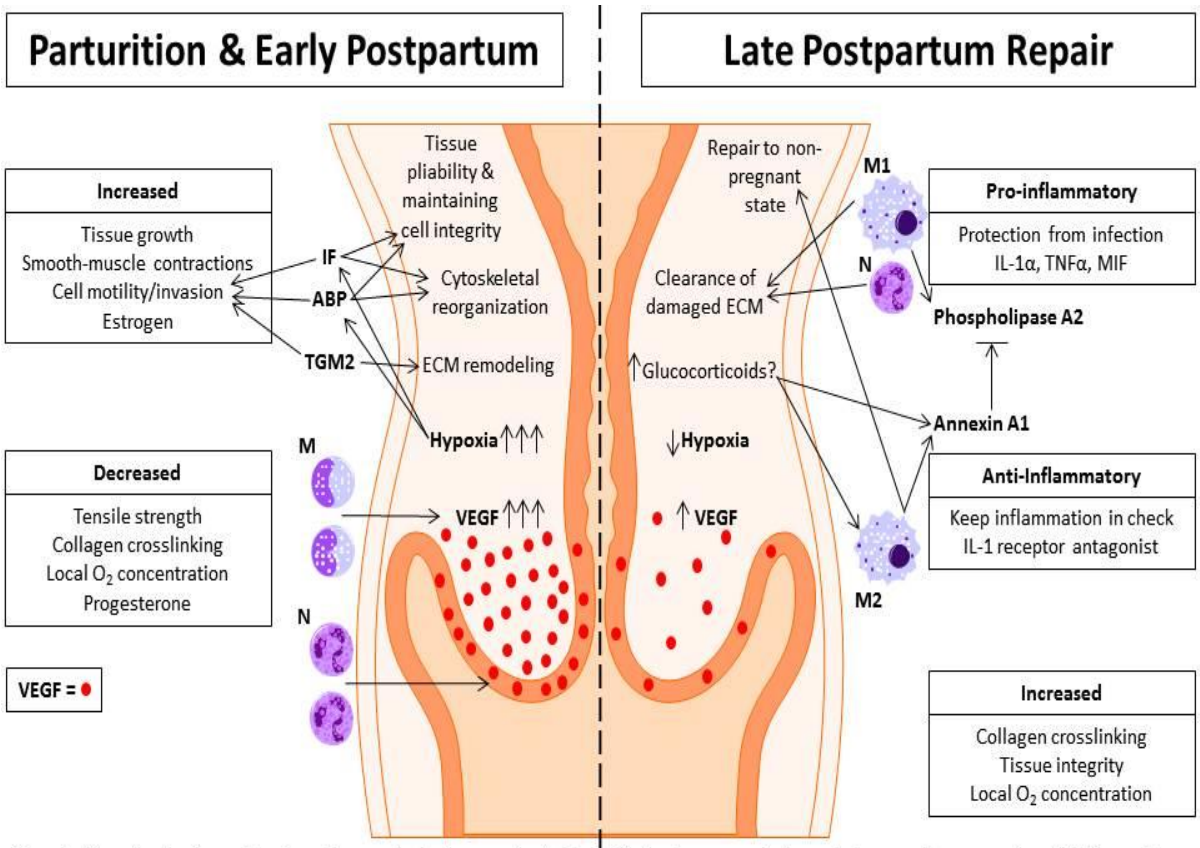

Figure 14: Proposed working model of postpartum repair cervical repair in the mouse.

Vita

Robert Lee Stanley was born on May 7, 1987 in Boone, North Carolina, to parents Jan and Steve Stanley with one older brother Christopher Drew Stanley. In the fall of 2004, Lee was awarded the rank of Eagle Scout, the highest ranking in The Boy Scouts of America, which less than 3% of scouts will achieve. Lee graduated from Watauga High School in 2005 and began his college career at Appalachian State University in August of that same year, with the hopes of pursuing a major in theater. Rapidly, he realized that a career in theater was not for him, and starting his sophomore year, he began taking biology courses. The next semester he declared as a Biology pre-professional major, with the hopes of attending medical school upon graduation. Lee graduated magna cum laude from Appalachian State University in December 2009, with a Bachelor of Science degree in Biology, pre-professional, with a minor in Chemistry.

Upon learning of his rejection from medical school, Lee contacted Dr. Chishimba Mowa about joining his reproductive biology research as a graduate student. In the spring of 2011, Lee began working towards his Master of Science degree in Cell and Molecular Biology, under the guidance of Dr. Mowa. While working towards his Masters, Lee was awarded the Chancellors Fellowship for graduate students, the GRAM research assistantship, several internal research grants, a nationally competitive research grant, attended several scientific conferences, traveled to South Africa on a clinical shadowing independent study, and was inducted into the Cratis D. Williams Society for outstanding graduate students. After graduation, Lee will continue reapplying to medical schools until he is accepted.